Specialist Committee on Cavitation

Final Report and Recommendations to the 25th ITTC

1 INTRODUCTION

1.1 Membership and Meetings

The 24th ITTC appointed the following members to serve on the Specialist Committee on Cavitation:

- Laurence Briançon-Marjollet (Chair), Bassin d'Essais des Carènes, France;
- Bong Jun Chang, Hyundai Maritime Research Institute, South Korea;
- Scott Gowing, Naval Surface Warfare Center, United States;
- Jan Hallander, SSPA, Sweden;
- Christian Johannsen, Hamburg Ship Model Basin, Germany;
- Takafumi Kawamura, University of Tokyo, Japan;
- Mohammad Saeed Seif, Sarif University of Technology, Iran;
- Erik van Wijngaarden, Maritime Research Institute Netherlands, The Netherlands; and
- William Zierke (Secretary), Applied Research Laboratory, The Pennsylvania State University, United States.

Mahammad Saeed Seif was unable to take part in the work of the committee. To aid the committee, Randy Riesterer of the Applied Research Laboratory at The Pennsylvania State University created the web site for the committee's cavitation survey and for the exchange of technical documents.

In performing their work, the committee held four meetings:

- Val-de-Reuil, France at the Bassin d'Essais des Carènes on January 17-18, 2006;
- Wageningen, The Netherlands near the Maritime Research Institute Netherlands on September 15-16, 2006 (following the International Symposium on Cavitation, CAV2006);
- Göteborg, Sweden at the SSPA on April 23-24, 2007; and
- Washington, D. C., United States at the Naval Surface Warfare Center on November 7-9, 2007.

1.2 Recommendations of the 24th ITTC

The 24th ITTC recommended that the Specialist Committee on Cavitation for the 25th ITTC address the following technology areas:

(1) Review the application of computational methods and new experimental methods to the prediction of cavitation, including cavitation dynamics and its influence on pressure fluctuations.

(2) Review advances in multiphase flow modeling of cavitation and its potential to predict inception, erosion, and induced pressure fluctuations.

(3) Review methods and develop guidelines for the prediction of cavitation and erosion damage for unconventional rudders or rudders behind highly-loaded propellers.

(4) Review methods of modeling the cavitation behavior of waterjets (inlets and pumps), including scale effects. De-

velop guidelines or procedures. Liaise with the Propulsion Committee.

2 CAVITATION SURVEY

The 25th ITTC Specialist Committee on Cavitation has been tasked to determine the status of cavitation modeling—with specific questions related to multiphase flow modeling, rudders, and waterjets. In order to fairly address the state of the art of cavitation modeling, the committee wanted to survey the opinions of the worldwide cavitation community. The committee developed survey questions in the following areas:

- Background Information,
- Cavitation Modeling Capability,
- Cavitation Experimental Capability,
- Rudder Cavitation,
- Waterjet Cavitation, and
- Summary Information.

2.1 Survey: Background Information

In June of 2006, the committee sent e-mail messages to 179 organizations—including ITTC members and other specifically-identified organizations who deal with cavitation—which asked them to go to a web site established by the committee and answer as many of the survey questions as they felt able to complete. 29 organizations from 14 countries completed the survey—with responses from Australia, China, Finland, France, Germany, Italy, Japan, The Netherlands, Poland, Russia, South Korea, Sweden, Turkey, and the United States.

2.2 Survey: Cavitation Modeling Capability

All but one of the responding organizations perform numerical and/or empirical modeling to predict cavitation performance. In the survey, the committee asked these organizations to quantify the accuracy of certain modeling techniques to predict various types of cavitation phenomena. In general, the responses indicated that the field of cavitation modeling is still not in a fully-matured stage of development, no matter which modeling technique is used. The empirical and potential-flow methods seem to have reached the stage where the accuracy is reasonable enough for trade-off studies, perhaps with the exception of predicting cavitation noise and cavitation erosion. The responding organizations rank the maturity of computational fluid dynamics (CFD) codes to be somewhat lower. Again, they feel that predicting cavitation erosion is the most difficult task.

Clearly, the organizations that develop CFD codes had more faith in the absolute accuracy of these types of codes than the organizations who are only CFD users. In general, the responding groups already feel that the CFD codes offer a good alternative to boundary-element codes. However, for all of the modeling methods, the survey indicated a large scatter in the judgment of the accuracy for cavitation predictions—which is not surprising, given the very limited availability of quantitative validation data.

For trade-off studies and scaling, all of the responding organizations utilize empirical modeling, based on both model-scale and full-scale test results—as well as theoretical formulations. For instance, empirical models for the inception of vortex cavitation are based on some modified form of the formula developed by McCormick (1962). Other empirical models attempt to account for nuclei population, thermodynamic effects, bubble interactions, pressure fluctuations, cavitation thrust breakdown, cavitation erosion, and cavitation noise. Some groups use a combination of empirical models and viscous CFD computations.

Most of the responding organizations utilize potential-flow methods, primarily for sheet cavitation. These groups used a mixture of their own codes, developed by other groups, and modified codes.

Sixteen of the 29 responding organizations that perform cavitation modeling, use commercial CFD software. For single-phase flow, many groups mentioned the use of commercial CFD codes for surface cavitation inception. The majority of the organizations that use commercial CFD codes mentioned that they use these codes with multiphase flow models, although a couple of groups linked these codes with models not available in the commercial CFD codes themselves. Some of the organizations mentioned success in predicting developed surface cavitation and cavitation thrust breakdown. However, little success was mentioned in predicting other cavitation phenomena. Finally, some of the groups mentioned the need for improved convergence time, robustness, and the resolution of the boundary between cavities and the water.

Seven of the responding organizations either develop their own CFD codes or use university-developed codes. These groups also develop their own multiphase flow models. The use of large-eddy simulation (LES) or detached-eddy simulation (DES) was also discussed to better resolve turbulent structures within the flow. Some groups use some mixture of CFD codes and potential-flow codes.

Clearly, many of the responding organizations feel that the use of CFD with multiphase flow modeling is important for cavitation predictions. While some of these computations are already becoming practical, the responding organizations felt that the use of CFD for other predictions—such as cavitation erosion, higher-order pressure pulses, and noise—will take several years.

2.3 Survey: Cavitation Experimental Capability

Most of the organizations that responded to the survey answered questions regarding their cavitation experimental capability, with 22 of the 29 organizations responding to at least some portions of this section of the survey. For the questions asking for comments or additional information, most of the organizations only provided short answers, and they mainly focused on the technical data (such as the size) of their facilities. Thus, the responding organizations provided very little information regarding new experimental techniques or new measuring equipment.

Of the responding organizations that perform cavitation experiments, all but one group utilizes a closed-jet-type of cavitation tunnel. Two groups use free-surface tunnels, while two other groups use depressurized towing tanks. For wake simulations during cavitation testing, the bigger facilities use full models, while the smaller facilities use dummy models or wire screens. When performing cavitation-inception tests, seventeen organizations simply use visual observation, while eight groups use video equipment, and eight groups use acoustic methods to determine inception.

To establish the water-quality conditions prior to cavitation-inception testing, nineteen of the responding organizations measure the gas-content level, with six of these groups using some device to measure the oxygen content, and four groups specifically responding that they used a van Slyke type of measuring device. Only six organizations stated that they measured the nuclei distribution—including just one large facility, two research facilities, two facilities where the method is under development, and one consultant group.

2.4 Survey: Rudder Cavitation

Only fifteen of the organizations that responded to the survey addressed the section on rudder cavitation. Nevertheless, of the fourteen groups that perform rudder cavitation tests, most of those organizations perform those tests with a rudder installed behind a propeller and acting in a non-uniform inflow. Depending on the capabilities of the organization, this non-uniformity is generated by wire screens of individually-adjusted mesh width, by dummy bodies, or by complete ship models. Only 17% of the responding organizations indicated the performance of rudder cavitation tests without any wake simulation.

The answers regarding the testing methods for cavitation assessment were even more uniform. 75% of the organizations rely on visual observation of the cavitation. Half of the organizations perform paint tests to judge the erosiveness of the cavitation, but almost all these groups only perform these paint tests as an addition to the visual observation. The reliability of this paint method may not be regarded as the best, primarily due to low local Reynolds numbers and the differing materials used for rudder models. The same holds for the use of high-speed video techniques—where 42% of the organizations use this special observation technique, but only to support the conventional visual assessment. This might be due to the lack of sufficient experience with the special kind of pictures gathered from high-speed cameras.

Most institutes with full-scale ship experience answered that almost all rudder cavitation phenomena (gap, sheet, and/or vortex cavitation), as well as the range of rudder angles where they occur, are under-predicted from the model test. Just a few organizations consider these values as similar, and no organization answered that these phenomena are over-predicted.

Twelve organizations responded to questions on modeling rudder cavitation. Most of these groups do not yet actively use viscous computational methods, in comparison with empirical and potential-flow methods. The use of multiphase-flow simulations to predict the unsteady cavitation behavior is rarely applied in the design stage.

Half of the responding organizations perform calculations for the rudder alone, but they use model testing or previous numerical computations to first obtain the flow downstream of the propeller and upstream of the rudder. The other groups consider the interaction between the propeller and the rudder in a single computation.

Two-thirds of the organizations design rudders based on the pressure distribution predicted without an analysis of the cavitation behavior. These groups do not regard the prediction of the cavitation behavior as relatively economic at the current time. Similarly, only two organizations even attempt to model cavitation erosion, probably because the physical mechanisms for erosion are still not clear.

2.5 Survey: Waterjet Cavitation

Not many organizations responded to the portion of the survey on waterjet cavitation. Of the 29 organizations that responded to the survey, only 11 organizations provided any input on waterjet cavitation—with nine organizations responding to the questions on experimental investigations, seven organizations responding to questions on modeling, and five organizations responding to both categories.

Regarding the experimental investigation of waterjet cavitation, the nine responding organizations all ran a variety of tests. Some reported on pump-loop testing to evaluate the waterjet pump alone—particularly for cavitation breakdown, but also with some flow-field measurements. More organizations reported on waterjet system tests, or on tests with the waterjet inlet alone. Most of the organizations simply provided very limited (or no) details. Only one waterjet manufacturer responded to the survey, and they clearly performed the most tests with the most types of measurements. For instance, they were the only responding organization who reported performing cavitation erosion tests. Most of the organizations reported on specialized tests—involving, for instance, detailed flow-field measurements, bubble-augmented waterjets, and totally-immersed waterjets integrated into a hydrofoil.

Six of the seven organizations that provided information regarding cavitation modeling for waterjets reported on the use of CFD to solve for the viscous flow field. These methods were used primarily to address cavitation inception—where some of the organizations also used empirical methods, potential-flow methods, and combined methods. One organization reported the use of a Burrill-like chart as an empirical method to model cavitation breakdown. The organization that did not report on using viscous CFD methods responded on the use of empirical methods for cavitation inception, breakdown, pressure fluctuations, vibration, and noise. Finally, only two organizations responded on the use of multiphase flow CFD methods: one for computing cavitation breakdown, and one for computing bubble behavior.

2.6 Survey: Summary Information

To complete the cavitation survey, the committee asked the various organizations to provide their view on the future of cavitation modeling—and to give them the opportunity to provide the committee with papers or reports that they felt were relevant to this investigation. Of the 29 organizations that responded to the survey, 16 organizations responded to the final summary question—and only three organizations uploaded any papers or reports.

A few of the responding organizations are currently working to couple their traditional potential-flow (or boundary-element) methods with more advanced methods in CFD, primarily viscous-flow solvers of the Reynolds-averaged Navier-Stokes (RANS) equations. However, several groups felt that the use of potential-flow methods for cavitation modeling would vanish in the next decade. Some of the responding organizations focused on the use of multiphase flow modeling in the context of a RANS formulation—primarily when addressing the prediction of bubble cavitation, cloud cavitation, and the interaction between the bubble dynamics and the flow field. They also mentioned the importance of understanding nuclei effects, and they stressed the use of these methods to better understand and predict scale effects.

Other responding organizations focused on the need to improve the modeling of unsteady cavitation—particularly to address cavitation inception, vortex cavitation, and cavitation erosion. These organizations mentioned unsteady RANS solvers, LES, and DES as promising methods for future modeling of unsteady cavitation. One responder also mentioned the possible need to model fluid/structure interactions. Depending on the cavitation problem that one needs to address, various cavitation modeling approaches will be used in the future, depending on both the physics of the problem and the available resources.

Even though most of the responding organizations that answered the final summary question focused on numerical cavitation modeling, a few responders felt strongly that model-scale testing still offers the best current method to model cavitation. In particular, they stressed the importance of using modern facilities to control and measure nuclei, using high-speed video, investigating basic cavitation and turbulence physics, measuring cavitation erosion, and using standard testing procedures. However, these responders did not disregard the use of numerical cavitation modeling. Instead, they advocated a more systematic approach of coupling experimental and computational models, especially the experimental validation of the computational models.

3 CAVITATION MODELING

The prediction of cavitation phenomena and the cavitation performance of marine vehicles and propulsors can involve either computational or experimental modeling methods. As summarized in the survey of the worldwide cavitation community, experts advocate the use of both computational and experimental methods, especially in providing experimental validation of computational simulations.

Verification and validation of computational simulations are the primary methods for building confidence in the simulations and quantifying this confidence. Oberkampf et al. (2004) provided a very objective and extensive description of verification, validation, and the predictive capability of all types of computational models. They describe verification as the assessment of the accuracy of the solution to a computational model, primarily by comparison with known analytical solutions. They describe validation as the assessment of the accuracy of the computational simulation by comparison with experimental data. Verification has no issue with relating the simulation to the real world—while for validation, the relationship between the computation and the real world is the issue.

Oberkampf et al. (2004) also state that verification and validation are ongoing activities that do not have a clearly defined completion point, primarily since computational models cannot be demonstrated for all possible applications and code options. They describe fundamental strategies for both verification and validation. Note that the validation strategy does not assume that the experimental measurements are more accurate than the computational results. The strategy only asserts that experimental measurements are the more faithful reflection of reality for the purposes of validation. For both verification and validation strategies, they discuss at length such familiar accuracy topics as the numerical algorithm, grid quality, boundary conditions, convergence, and experimental uncertainty.

In the following sections of this report, the 25th ITTC Specialist Committee on Cavitation will examine current cavitation modeling used by organizations to impact design, as well as the state-of-the-art of multiphase flow cavitation modeling. Then, the committee shows how organizations are using these varied cavitation modeling methods to address cavitation issues on rudders and within waterjets.

Before proceeding, the committee will define the primary parameter used to quantify or categorize cavitation performance—namely, the cavitation number (or cavitation index),

$$\sigma = \frac{p_{ref} - p_v}{\frac{1}{2}\rho V_\infty^2}. \tag{3.1}$$

In this equation, p_{ref} is a reference static pressure, p_v is the vapor pressure (usually at the bulk temperature of the fluid), ρ is the fluid density, and V_∞ is the freestream velocity (which is usually the ship speed, V_{ship}). Defined similar to a static-pressure coefficient, one can essentially think of the cavitation number as the fluid's reserve of static pressure before cavitation. As long as this reserve is greater than any drop in the local static-pressure coefficient, no cavitation will occur.

4 CURRENT CAVITATION MODELING METHODS

In reviewing the varied cavitation prediction methods, the 25th ITTC Specialist Committee on Cavitation began by examining new experimental methods that organizations have employed to investigate cavitation phenomena. Following this experimental review, the committee examined computational methods that organizations are currently using to impact design—methods that include empirical methods, potential-flow methods, and RANS solvers without multiphase flow models. The review of these modeling methods is representative of current methods used by many organizations, but it is by no means exhaustive.

4.1 Experimental Techniques

Much of the recent development of experimental methods involves non-intrusive optical techniques for velocity measurements—which impact cavitation modeling, even for measurements in non-cavitating flow fields, such as propeller flows upstream of rudders. Some acoustic methods have also become popular for velocity measurements, but these are typically limited to hull flows or boundary-layer measurements in ship motion tests. Additional improvements of experimental techniques that impact cavitation modeling include photography and video measurements, unsteady pressure measurements, nuclei measurements, and cavitation erosion measurements.

Laser Doppler Velocimetry. Modern non-intrusive optical methods for measuring flow fields have improved investigations of cavitation phenomena. Laser Doppler velocimetry (LDV) is a well-proven technique that accurately obtains mean-flow and turbulence statistics at single points in a flow field. While LDV techniques can resolve spatial structures, they can require long data-collection times. Also, unsteady movement of the spatial structures can be *smeared* out while averaging data at a single point and can be confused with turbulence statistics.

Fry [2007] and other researchers have improved the ability of LDV measurements to survey flow fields by employing *scanning* techniques that resolve mean flows, velocity variations, and turbulence data with increased efficiency and greater spatial resolution—as opposed to the classic *move-collect, move-collect* survey motions. Scanning techniques move the probe volume continuously through the flow field and collect data at the same time. The time required for data collection is shorter because the average velocity at each scan location is an independent measurement of the time-varying velocity, not a duplicate measurement of an unchanged velocity. Scanning techniques require more detailed data analysis, to remove the scanning velocity —for example—and require data collection time scales that are shorter than the velocity time scales. But the overall data collection time can be shortened, which is important for towing-tank tests that provide wake data for propeller calculations. Measurements can also be made closer to reflective boundaries because the residence time per measurement is shorter, avoiding signal saturation in the receiving optics—giving an advantage, for instance, for waterjet surveys in closed flows.

Particle Image Velocimetry. Particle image velocimetry (PIV) measures the instantaneous global velocity field on a plane. The resulting instantaneous *snapshots* of the flow field offer advantages over LDV. Stereo PIV (SPIV), defocused PIV (DPIV), and holographic PIV (HPIV) have extended the traditional planar PIV into three dimensions. These techniques use multiple measurement planes or spatially-dependent focal planes to resolve flow fields in volumes.

Longo et al. [2004] presented a good survey of the variations of PIV measurements. PIV has increasingly been used for the study of propeller wake and propeller/hull interaction flows, because of its efficient ability to capture the structures in the flow—both the steady-state flow and the time- or spatially-varying flow. The increasing resolution of charge-coupled device (CCD) camera sensors and faster framing rates are enabling higher data rates with finer spatial scales, and improved data processing techniques are making PIV data more accurate. As discussed by Atsvapranee et al. [2007], PIV has become an accepted method for velocity field measurements and is now becoming more standard.

Investigators such as Di Felice et al. (2004) and Calcagno et al. (2005) have used PIV for propeller flow measurements. More recently, Felli et al. (2006) have performed a unique investigation that used PIV to study unsteady pressures. They used a rake of hydrophones to correlate pressure fluctuations in the wake field of a propeller with PIV measurements of the local radial and tangential velocity vectors. These data were aligned with the propeller blade position to study the blade wake evolution downstream and features of the wake within the propeller slipstream. Figure 4.1 shows examples of these correlations.

Although the experiment of Felli et al. (2006) is conducted in non-cavitating conditions, the technique is noteworthy for its applicability to measure in-flow pressure pulses in phase with the propeller. Such a technique can be useful for studies of pressure-pulse propagation and evolution near the hull. Power spectral density data show the spatial evolution of the amplitude of the dominant frequencies of the flow field, and high turbulence intensities correlate well with the standard deviation of the pressure coefficient. This technique offers simplicity for adding pressure measurements to an existing PIV setup, but it requires accurate coordination of data collection from different systems (pressure sensors and PIV). The data were corrected for background flow and noise levels, but the errors introduced by the physical presence of the hydrophone rake were not addressed. Di Felice et al. (2004) emphasized the error estimates of PIV as applied to a propeller wake field.

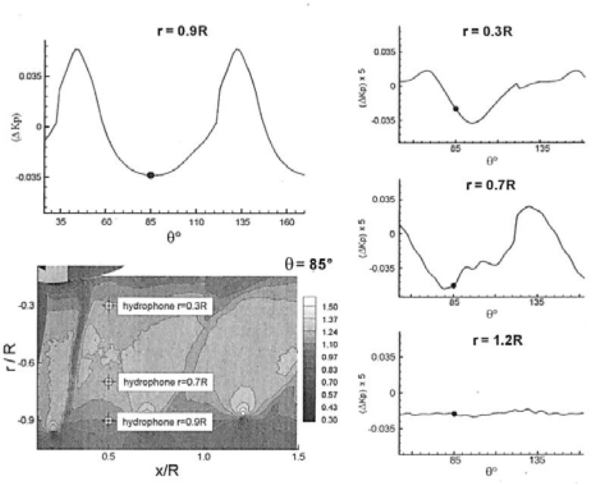

Figure 4.1 Correlation of velocity field and pressures from Felli et al. (2006), at J=0.88.

Foeth and van Terwisga (2006) used time-resolved PIV to measure velocities around a fluctuating sheet cavity on a hydrofoil. By using particles that fluoresce at wavelengths different than those from the illumination sheet, the reflections of the cavity were filtered out, enabling resolution of particle traces close to the edge of the cavity. These data are difficult to measure, but important to understanding cavity cloud dynamics and verifying numerical predictions.

Calcagno et al. (2005) used SPIV to investigate a propeller wake behind a ship model in a large free-surface tunnel. They measured the blade boundary layers, vorticity sheets, and hull wake. For measurements near the propeller, the propeller image was subtracted out of an ensemble average of the SPIV images to remove the propeller reflections from the images and improve the data rate. The camera positions are unique, in that the camera angles are not symmetric. One camera outside the tunnel was used with a second underwater camera, offering a setup from one tunnel side only.

Photography and Video Measurements. Boroscopes are becoming popular for full-scale cavitation viewing, as discussed by Carlton and Fitzsimmons (2006). Recent improvements have been in lower light loss optics, synchronization capability of the images with data, and higher frame rates up to 1,500 frames/second. Increased data transfer rates with newer computer technologies should allow even faster frame rates in the future. Higher frame rates allow correlations of complex interactions of cavities during the passage of a single blade flow field, not just visualization of cavity patterns on the blade itself. Recently, Oweis and Ceccio (2005) have shown that vortex interactions can lead to inception before it occurs within the structure of a single vortex; hence, visualization of cavity interactions becomes increasingly important for inception and scaling studies. Cavity cloud behavior is important for understanding hull pressures. In attempting to understand cavity phenomena during maneuvers, one can also make use of higher-frame-rate boroscope cameras.

Higher frame rates allow better detection of inception via changes of small white spots that may not appear in synchronized, one-shot-per-revolution videos. This improved detection is especially important for intermittent cavitation, as shown by van der Hout et al. (2006). Carlton and Fitzsimmons (2006) also pointed out that non-periodic cavitation revealed with high frame rates at full scale can make Fourier analysis of hull pressures difficult because of the cavities' non-periodic behavior.

Measurement of the extent of blade surface cavitation has been used to validate various computational schemes. Simple photography/video provides information on the cavity area, but this approach has optical issues because of the viewing angle of the camera. As an improvement to this technique, Pereira et al.

(2004) used the *warping* transformation to correct a perspective image of a propeller blade to its planform view. A spatial matrix is used to transform coordinates on a propeller blade to the perspective view from a camera outside of the cavitation tunnel. The warped (or corrected) view is then analyzed for cavitation area coverage using common optical contrasting and thresholding techniques. The warping calibration is applied to well-defined sections of the blade, not just the blade outline, and this makes a more accurate correction of the image. Figure 4.2 illustrates this warping technique. The measured cavitation areas agree fairly well with inviscid boundary-element methods used for prediction of the cavity coverage. Future work will address measurement of the cavity volume. The measurement of volume fluctuations is important to validating the prediction of pressure pulses and monopole sources for low-frequency blade-rate noise.

Unsteady Pressure Measurements. Wang et al. (2006) demonstrated the use of a polyvinylidine fluoride (PVDF) sensor array to measure the near-field pressures of a cavitating bubble. These kinds of sensors have a much higher frequency response than standard piezoelectric transducers. Arndt et al. (1997), Soyama et al. (1998), and Shaw et al. (2000) have used PVDF sensors in cavitation research and shown good correlation of pulse height with erosion rate. Laser micro-machining is used to etch 4.5-mm x 5.0-mm sensors onto a patch. While the sensors are aligned in one dimension, a two-dimensional array appears to be possible. A buffer circuit is developed to provide low impedance output signals with a wide dynamic frequency range (>10 MHz). Calibrations show consistent sensitivity across the sensors with little cross talk. Peak pressures in the order of >10 MPa are measured, but these values are averaged over an area and are much lower than the peak pressures that cause erosive pitting as—shown by Philipp and Lauterborn (1988). It should be possible by making an array of these sensors, and using phase correlation techniques, to locate pressure pulses in space.

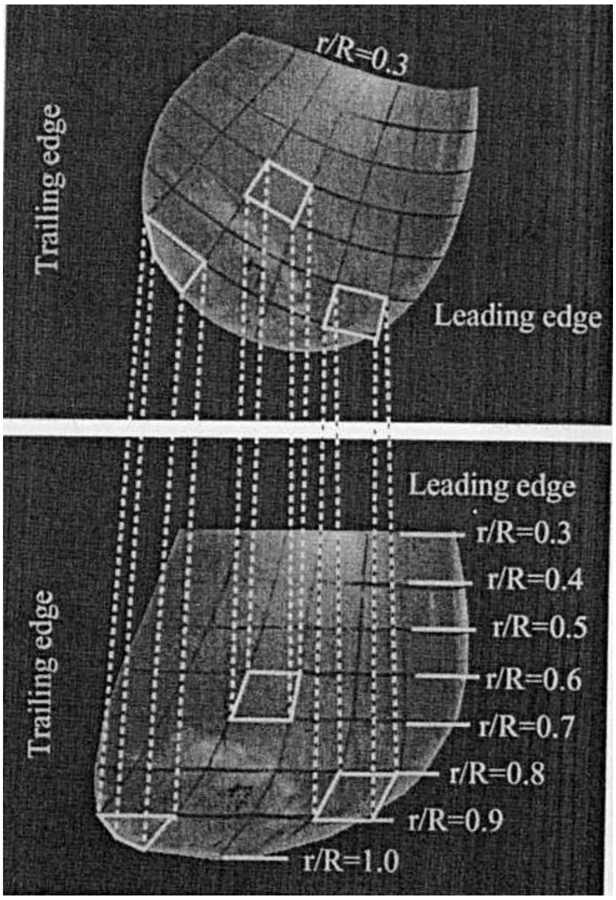

Figure 4.2 Illustration of warping technique used by Pereira et al. (2004).

Nuclei Measurements. Defocused techniques using lasers are being studied for bubble or droplet size measurements. In one variant, interference patterns between reflected and refracted rays from spherical scatterers appear within out-of-focus planes behind a lens. Analysis of the spacing of the interference fringes and the distance between the focus and image planes determines the bubble size.

Damaschke et al. (2006) used two coherent light sheets in the same plane to allow the bubble positions to be determined in the out-of-plane direction from the two resulting sets of interference patterns, as shown in Figure 4.3. These techniques are still under development, but they offer advantages to standard phase Doppler anemometer (PDA) techniques—for which sample volume definition and data rates can be a problem, especially in large or sparse particle fields. The analyzed images must be bubbles, however, because interference is required from the reflected and refracted rays.

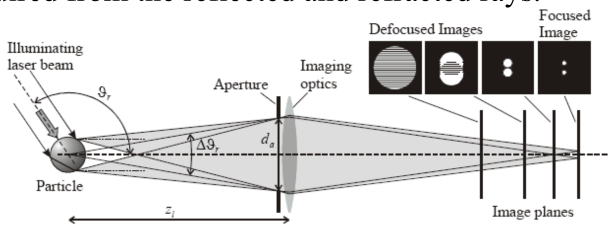

Figure 4.3 Schematic of the interferometric-bubble-sizing method of Damaschke et al. (2005).

Palero et al. (2005) adapted the defocused technique by using two laser sheets to produce two first-surface reflections that discriminate spherical from non-spherical scatterers, where they assumed that the spherical scatterers were bubbles. Holographic PIV can also use interference patterns within out-of-focus planes for bubble sizing, or simply discriminating bubbles from particles by resolving the two specular reflections for bubbles. Straightforward optical examination at high magnification can still be used, but this method places demands on the resolution of the system.

Researchers have recently adopted acoustic techniques for nuclei measurements—non-intrusive techniques which interact only with bubbles. In conjunction with this type of technique, Chahine and Kalumuck (2003) developed inverse scattering algorithms that use pulse signals to provide bubble sizes and concentrations.

Cavitation Erosion Measurements. Erosion measurements are made using a variety of techniques. The classical pit-count-rate method evaluates surface erosion and can be used to rank different materials for erosion resistance or rank cavitation intensities for the same material. Optical profiling of the pits has been used to extend this method for estimates of the lost volume of material. Patella et al. (2000) used laser profiling to map the surface contour of erosion pits. Bachert et al. (2005) used a rotating disc with holes to create erosive cavitation on copper samples. A novel white light interferometry technique measured the depth profiles of eroded areas, and the resultant volumes compared well to a direct mass loss measurement. The results also showed qualitative agreement with pit counts using CCD cameras. Escaler et al. (2007) have shown good correlation of acceleration impulse with pit rate for unsteady cloud and sheet cavitation. The accelerometer signals are band-passed filtered at the modulated frequency of the cavity cloud collapse, and the resultant signal levels are well-correlated with pitting rate.

4.2 Computational Prediction Methods

Along with experimental methods, most organizations also use different computational methods to predict cavitation performance. These computational methods include empirical methods, potential-flow methods, and RANS solvers without multiphase flow models. The use of RANS solvers with multiphase flow models will be discussed in Section 5 of this report.

Empirical Methods. The cavitation survey showed that some organizations feel that cavitation is still primarily an experimental discipline, where testing still offers the best current modeling method. Thus, experimentalists have acquired a large amount of cavitation data, at different scales, and used these data in conjunction with theoretical formulations to develop empirical methods to model cavitation. These methods are still indispensable for designers to account for the effects of cavitation, especially at early stages of a design.

As mentioned in response to the cavitation survey, many organizations use empirical models for the inception of vortex cavitation which are based on some modified form of the formula developed by McCormick (1962). For instance, Shen et al. (2001) applied a log law to vary the thickness of the boundary-layer thickness with Reynolds number—and the resulting scaling exponent is dependent on the Reynolds numbers of the model and prototype scales.

Burrill (1943) and Burrill and Emerson (1963) developed the Burrill chart as an empirical method to assess the tendency of cavitation thrust breakdown for a propeller. Breakdown is typically negligible for cavity coverage less than 10% of the back face of the blade. Recently, Black (2007) analyzed data from five propellers with modern blade sections and proposed an empirical formula for the onset of cavitation thrust breakdown that relates a thrust-loading coefficient to the cavitation index. Figure 4.4 shows the predictions using his method. The resulting formula includes a correction for low-order harmonic inflow variations typical of shaft inclination angles, and is close to the 15% backface cavity coverage criterion of the Burrill chart. Levels of cavitation thrust breakdown to 5% are found to be tolerable because the lost thrust can be recovered by increased propeller speed, in spite of the slight increase in cavitation. Beyond 10% loss, the thrust cannot be recovered.

Van Rijsbergen and van Terwisga (2000) reviewed existing criteria for maximum thrust density on open and ducted propellers. The maximum thrust capability of a given propeller is determined by two criteria: a non-dimensional thrust-density criterion and a non-dimensional tip-speed criterion. Dimensional equivalents of these two criteria are less reliable because they show too large of a dependency on shaft immersion and efficiency. The thrust capability of a propulsor is dependent on the wake field, the propulsor type, and the propulsor design—giving parameters that should be included in any empirical model. The existing empirical model shows a good correspondence with experimental results on conventional propellers, when the maximum thrust capability is defined at the point where a 2% thrust cavitation breakdown is reached.

Potential-Flow Methods. The development of algorithms to solve the RANS equations and perform viscous CFD simulations—as well as the necessary computer power—has only recently impacted cavitation modeling. Previously, hydrodynamicists have used the assumptions of inviscid and irrotational flow to develop potential-flow methods to solve for the flows in the vicinity of ship hulls, propellers, rudders, and other geometries of interest. For cavitation modeling, these hydrodynamicists have developed lifting-surface, panel, vortex-lattice, or boundary-element methods that model the cavities, as well as the geometry. One can also solve the inviscid Euler equations, without the assumption of irrotational flow.

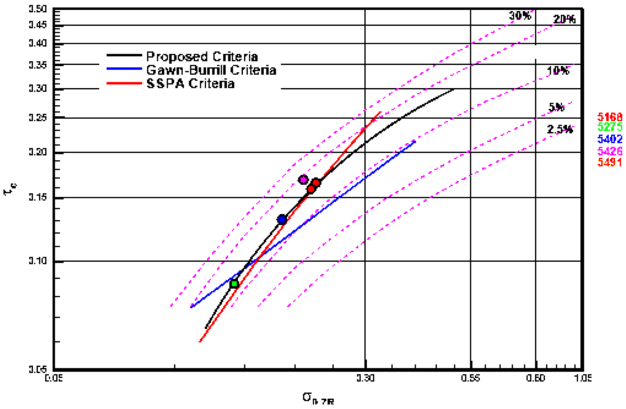

Figure 4.4 Cavitation thrust breakdown prediction by Black (2007).

Because of their efficiency, these potential-flow methods are still used for propeller design and for predictions over a range of flow and cavitation conditions. These methods can address non-uniform inflows and predict fluctuating forces and pressures produced by sheet cavitation. Several researchers, including Kinnas et al. (2007), have developed corrections for viscous-flow effects by using RANS predictions for the incoming wake and vorticity fields or by incorporating boundary-layer integral solvers or viscous empirical corrections into the potential-flow methods.

Lee and Kinnas (2004) developed a boundary-element method (BEM) that couples calculations for tip vortex cavitation with fully unsteady sheet cavitation on a propeller blade. The predicted shape of the tip vortex cavitation compares well with elliptic foil results, and the method is applied to a propeller tested in a ship wake. The resulting blade cavity shapes match experiments much better near the tip region with addition of the calculated tip vortex cavitation. Without the calculated tip vortex cavitation, the predicted sheet cavities are too large. Lee and Kinnas (2004) also predict the resulting cavitation forces.

Takekoshi et al. (2005) used a vortex-lattice method (VLM) for optimization of a propeller design in a non-uniform wake by evaluation of the time-dependent pressure distribution and cavity volume development. By shifting the loading distribution more towards the rear of the chord, they reduced the cavity volume, while maintaining the same overall loading distribution. Experiments confirmed the predicted trends from the design optimization. The reduced cavitation volume reduces the low-frequency, blade-rate components and also reduces higher-frequency noise associated with tip vortex cavity bursting. This decrease was attributed to the reduction of the tip vortex cavity volume. In addition, they achieved a higher net efficiency for their new propeller design.

As demonstrated by Takekoshi et al. (2005), the efficiency of potential-flow codes combined with faster computers has allowed designers to apply optimization schemes to complex problems, including problems involving cavitation. Takekoshi et al. (2005) used their VLM with a cluster of personal computers to optimize blade section and pitch distributions for a cavitating propeller in a non-uniform wake. Cavitation and efficiency are two parameters that typically cannot be varied independently in optimization schemes. Han et al. (2006) evaluated various optimization schemes for maximizing propeller efficiency, while simultaneously meeting a criterion for the hull pressure fluctuations.

Falcao de Campos et al. (2006) studied the influence of the frequency on the partial-sheet cavitation behavior within the gust of a two-dimensional hydrofoil. Using a boundary-element method, they found that the effect of the wake peak on the cavity length can be nonlinearly significant.

Single-Phase RANS Methods. The cavitation survey clearly showed that most organizations involved with problems associated with cavitation currently use CFD—either using their own codes, university-developed codes, or commercial codes. These viscous-flow codes solve the Reynolds-averaged Navier-Stokes (RANS) equations. Even without including any multiphase flow models which will be covered thoroughly in Section 5 of this report—these RANS solvers have proven valuable for evaluating cavitation inception, especially for the inception of surface cavitation. In addition, some organizations use RANS solvers in conjunction with empirical modeling and potential-flow modeling.

To show the accuracy of computations to an engineering level, Li (2006) compared RANS computations of the flow through a highly-skewed propeller, over a full range of advance ratios, to open-water powering data, PIV data, and the results of paint tests and cavitation-inception tests. Using a commercial code, he showed that the minimum pressure coefficient on the blade surface was sensitive to grid refinement. Within the tip vortex, he showed that the computational and experimental results for the inception cavitation number differed by 7%, but he urged caution for this type of computation and the strong sensitivity to grid density. Others have shown issues related to the turbulence model and the basic unsteadiness of the tip vortex and its minimum pressure.

Bulten and Oprea (2006) used a single-phase RANS solver to study the effects of grid refinement and turbulence modeling on propeller tip-vortex cavitation inception at model and full scale. The results show robustness, provided that they did not use the overly-dissipative k-ε turbulence model. The exponents derived for the McCormick (1962) type of scaling from the predictions show smaller exponents than those usually found experimentally, similar to the trends from the empirical model of Shen at al. (2001).

Dreyer et al. (2006) used a single-phase RANS solver in developing a multipoint shape-optimization method using the continuous adjoint approach. They obtained an optimized hydrofoil design to improve cavitation-inception performance at off-design conditions. Then, they analyzed the optimized hydrofoil and the original baseline hydrofoil numerically using a RANS solver and experimentally in a water tunnel. Both analyses showed that the shape-optimization method successfully reduced the cavitation number for the optimized hydrofoil at off-design incidence angles and widened the *cavitation bucket*.

4.3 Cavitation Noise and Pressure Fluctuation Prediction Methods

In reviewing the current cavitation modeling methods, the 25th ITTC Specialist Committee on Cavitation specifically set out to investigate how these prediction methods address cavitation dynamics and its influence on pressure fluctuations and noise.Dang (2004) compared pressure pulses for flat versus triangular pressure profile blade sections passing through a simulated sinusoidal wake by calculating cavity volume time derivatives. The results showed equivalent values. He focused on the varying propeller profiles to change pressure pulses, leading-edge cavitation, and leading-edge vortex separation.

Ligtelijn et al. (2004) compared model- and full-scale pressure fluctuation data for five different ships, including two with nozzle/propeller propulsors. Calculations of the pressures were made with three sets of programs from two different laboratories. Additionally, the calculations and model tests were conducted with the full-scale conditions, as input to remove the effects of variations of the full-scale-trial and model-test conditions. For the Azipod propulsors, Ligtelijn et al. (2004) showed good correlation between the full-scale and model-scale data—where the calculations either slightly over-predicted the first blade-rate tone or gave very accurate predictions, depending on the method. The nozzle propulsor results showed poor agreement between model-scale data and predictions, with the predicted cavitation being too strong. Another nozzle-propeller test showed over-predicted fluctuations for the same reason, but the fully-wetted pressures were under-predicted, and the difference were attributed to reverberant characteristics of the nozzle. For this case, the simple reflection coefficient of two for a flat, solid boundary may be too small. Such propeller arrangements may require reverberation estimates that can be very frequency dependent.

For container ship correlations, Ligtelijn et al. (2004) showed over-predictions of the pressure pulses, primarily because of excessive cavitation calculated using model wakes, which were not sufficiently corrected for scale effects. The absence of good tip vortex modeling also caused discrepancies between the calculated and measured data. Ligtelijn et al. (2004) also revealed the importance of discriminating the pressure pulsations from the passage of the blade volume and the unsteady force pressure pulsations from the cavity volume pressure pulses. In the case where the source strengths were similar for these two phenomena, the phase relationship becomes important in determining the net amplitude on the hull. Low-amplitude pulses can be the lucky result of phase cancellation and not the result of a good design.

Lee and Chen (2005) predicted propeller cavitation and pressure fluctuations with and without hull interaction effects by coupling an Euler solver with a vortex lattice method and comparing the results to a RANS code coupled to the same VLM. The hull interaction had a very strong effect for the first blade rate and indicated the strong influence of hull interaction on the propeller inflow.

Kehr and Kao (2005) calculated far-field noise of a cavitating propeller from cavitation and unsteady forces. They based the cavity volume on unsteady lifting-surface calculations, mixed with dipole models of unsteady forces. Far-field results showed that cavity volume noise can be replaced by a point source on the blade, but near-field results require the noise source distribution.

Seol et al. (2005) computed low-frequency noise from a cavitating propeller in a wake. Potential-flow panel methods predicted the strengths of monopole cavity volume fluctuations and the dipole source strengths from unsteady blade forces. The cavitation volume histories compared well with experiments, as shown in Figure 4.5. The sources were summed using a time-domain Ffowcs-Williams-Hawkings formulation to estimate the far-field acoustics. The high-frequency sources from collapsing cavitation were ignored. Further research is needed to predict noise at those frequencies.

Van Wijngaarden et al. (2006) proposed an inverse BEM that models the propeller as a combination of monopole, dipole, and quadrupole sources to model cavity volume fluctuations, thrust loading, and blade thickness, respectively. The advantage of this technique is the ability to model the propeller-induced hull pressure field with sparse hull pressure measurements, and discriminate the cavitating and non-cavitating sources.

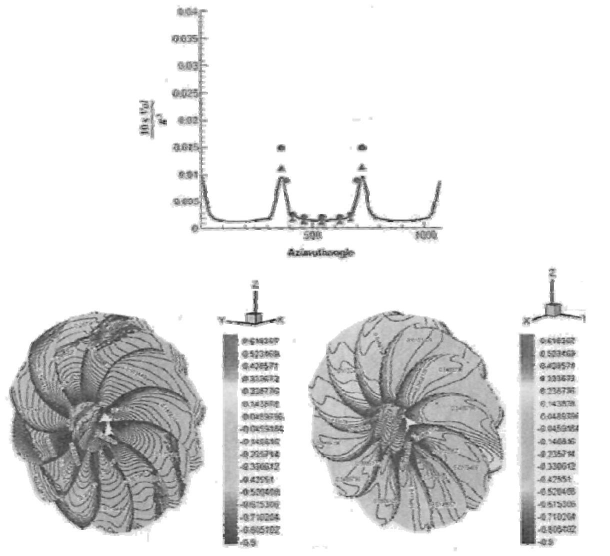

Figure 4.5 Comparison of calculated and measured pressure contours and cavity volumes by Seol et al. (2005).

Abel (2006) used a vortex lattice method, with a correction scheme to calculate the effective wake and to calculate pressure pulses arising from cavitating and non-cavitating sources on a series of propellers. The results were empirically correlated using model pressure test data to derive more accurate predictions. The purpose of the calculation procedure is a scheme to quickly predict pressure fluctuations at the early stage of a propeller design study.

Koronowicz and Szantyr (2006) proposed a computational technique (KAWIR) for the prediction of tip vortex cavitation and its noise spectrum. They addressed both explosive, critical nuclei growth and bubble oscillations. The isobars of the vortex were calculated, and then they were merged with a nuclei distribution to determine the number of bubbles undergoing explosive growth via their critical pressure. The pressure-field time histories from each bubble were summed to determine the sound pressure spectrum. For the case of bubbles merging in a segment of the vortex core and making an elongated bubble, Koronowicz and Szantyr (2006) replaced the vortex segments with equivalent point sources to calculate their contribution to the overall spectrum. The bubble trajectories were not corrected for the vortex flow field, and the bubbles were treated as singular events with no interactions. While this general approach to calculations of bubble dynamics in a tip vortex is not new, Koronowicz and Szantyr (2006) claimed that the model of a single vortex from a propeller tip is inferior to a double layer model that strongly affects the tip vortex conditions. They claimed that the open propeller designs were vortex-cavitation free up to 30 knots, but they did not show any experimental data.

5 MULTIPHASE FLOW CAVITATION MODELING

While current cavitation modeling methods have been used to impact design, these methods have a number of limitations, particularly in modeling multiphase flow. To address advances in multiphase flow modeling of cavitation, the 25th ITTC Specialist Committee on Cavitation has proceeded from the definition of multiphase flow modeling as the science of numerically modeling cavitating flows on propellers, rudders, and appendages by means of CFD codes that involve void-fraction modeling or at least two phases. Thus, potential-flow methods—such as boundary-element methods of two-phase flows—are excluded from this section of the report. (These methods were included in the previous section of the report.)

The remainder of this section includes an overview of the field of multiphase CFD and a literature review of material that researchers and users have reported since 2003. In addition, this section includes a discussion on the use of LES and DES to better resolve turbulent structures and improve the modeling of unsteady cavitation.

5.1 Multiphase Flow Modeling

Many numerical models of cavitation have been proposed in the last three decades. In early models, it was assumed that the cavity is a vapor film in which the static pressure is constant. Models of this kind have been used mainly on the assumption that the flow is irrotational, and they have been practically applied to attached sheet cavitation or supercavitation. However, the range of application has been limited because these traditional methods usually require somewhat empirical or *ad-hoc* treatments at the leading and trailing edges of the cavity. Recently, with the increase of computational power and improvement of turbulent flow simulation methods, more general and flexible *multiphase flow models* have attracted attention.

The multiphase flow modeling of cavitation can be distinguished from the traditional approach in that cavitating flows are modeled with a continuum, variable-density fluid. The traditional interface-tracking approach has been used mainly in combination with methods based on potential-flow theory, whereas the multiphase-flow approach is more often used in combination with RANS simulations—or, very recently, with DES and LES. The advantage of multiphase flow cavitation models over the traditional interface tracking approach is the flexibility of the framework. Thus, they offer a better perspective of modeling more details of cavitation and its consequences. Whether this type of modeling is good enough for practical purposes is still to be proven.

The multiphase flow model is based on the concept of phase averaging. For example, if cavitation is considered as a two-phase flow (some researchers take non-condensable gas as a third phase), one assumes that, at a given instant, the fluid in an arbitrarily small volume centered at a certain point in space is a homogeneous mixture of vapor and liquid. The mixture fluid properties, like mass density and dynamic viscosity, are an average of the liquid and vapor properties, based on the local constitution at that instant, governed by a nondimensional scalar phase fraction parameter, which is either the volume fraction of vapor (α_v) or the volume fraction of liquid (α_l), where $\alpha_l = 1-\alpha_v$ in a two-phase flow.

One approach is now to derive the mixture density (and thereby the volume fraction) from the instantaneous pressure via an artificial equation of state. This type of model is also referred to as a barotropic model. It assumes that bubbles instantaneously respond to the global pressure variations. It also implies that an equal-pressure surface in the flow is an equal-density or equal-phase-fraction surface.

In another, more extensively pursued approach, the computation of the cavitating flow is based on the solution of the equations for mass and momentum conservation of the mixture fluid (including a turbulence model), together with a transport equation for the volume fraction parameter. The latter equation must have creation and destruction terms to model the evaporation and condensation processes. As a matter of fact, the formulation of these source/sink terms distinguishes the various cavitation models which have so far been proposed in this category. In some versions, the formulation has a bearing on the Rayleigh equation for bubble dynamics; in other versions, it has simply been tuned to the behavior of cavitation observed in experiments.

In the numerical solution of cavitating flows, several problems are encountered and, from publications, it is not always clear how they are resolved. In that sense, there is considerable similarity with turbulence modeling. Moreover, the choices on spatial and temporal resolution seem to be important. But with the increase of the resolution in space and time, the computation time goes up dramatically. On the other hand, it is difficult to judge the performance of a given cavitation model, as long as the solution has not been shown to be independent of time step and grid spacing. This is to say that a lot more work has to be done to arrive at best practice guidelines for numerical modeling of cavitation.

5.2 Review of Recent Literature on Multiphase Flow Cavitation Modeling

Multiphase flow modeling of cavitation is a very active research area, and many research groups—mainly in Europe, the United States, and Japan—are engaged in this research. In the next section, the committee reviews the recent advances of these models, and their potential to predict cavitation inception, erosion, induced pressure fluctuations, and thrust breakdown.

Fundamental Studies and Validation on Simple Geometries. A significant amount of effort has been made so far to investigate the validity of multiphase flow cavitation models. In many studies, cavitating flow around two-dimensional simple geometries, such as foil sections, have been simulated and compared with experimental results. In 2003, during the Fifth International Symposium on Cavitation (CAV2003) in Osaka, Japan, the organizers held an interesting session. The objective of the session was to compare computational results on a common test case. The subject chosen in the session was cavitating flow over a two-dimensional hydrofoil for which experimental data were not yet available. Figure 5.1 shows the geometric configuration of this problem.

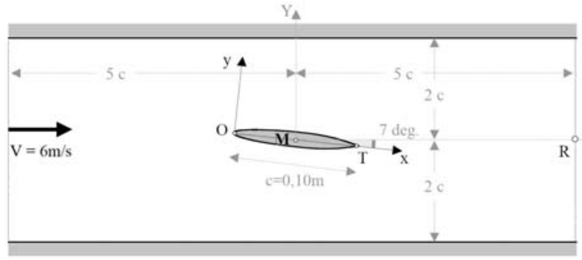

Figure 5.1 CAV2003 hydrofoil test case.

Participants were requested to simulate the flow at the non-cavitating condition and at two cavitation numbers, $\sigma = 0.4$ and 0.8. Seven out of the eight papers presented in the session used multiphase flow modeling. Qin et al. (2003), Pouffary et al. (2003), Saito et al. (2003), and Coutier-Delgosha and Astolfi (2003) used the state-law approach—while Wu et al. (2003), Kawamura and Sakoda (2003), and Kunz et al. (2003) used either the bubble two-phase flow model or a heuristic model. Although experimental results were not presented, the computational results suggested that a periodically-collapsing sheet cavity appears at $\sigma =$ 0.8 and that relatively stable supercavitation occurs at $\sigma =$ 0.4. While most participants predicted this qualitative feature, Figures 5.2 and 5.3 show that the computed time-averaged quantities were quite scattered.

It should be noticed that those computed quantities are influenced not only by the cavitation model, but also by various computational conditions such as the turbulence model, the grid resolution and quality, the discretization scheme, and so on.

More recently, Patella and Reboud (2006) and Rolland et al. (2006) have shown detailed comparison of the computation using the barotropic-state-law model and an experiment for a cavitating flow in a Venturi. Also, Takekoshi and Kawamura (2006) have carried out a systematic validation of the full cavitation model developed by Singhal et al. (2002) for cavitating flows over various hydrofoils. These researchers showed reasonable overall agreement between the simulation and the experiments. However, Takekoshi and Kawamura (2006) suggested that the reliability of the simulation is dependent on other conditions, such as the angle of attack or the hydrofoil section. As for the turbulence model, Coutier-Delgosha et al. (2003a) and Xiong et al. (2006) have pointed out that the predicted cavity patterns are significantly influenced by the choice of the RANS models. Recently, Wosnik and Arndt (2006), Persson et al. (2006), and Wang and Ostoja-Starzewski (2007) applied LES to cavitating flows.

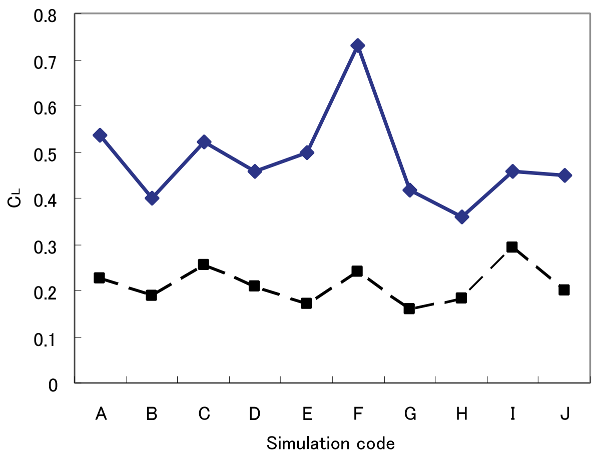

Figure 5.2 Comparison of the computed lift coefficients of the CAV2003 hydrofoil at two cavitation numbers (where σ = 0.8 are the blue diamonds and σ = 0.4 are the black squares).

While most validations have been two dimensional, Kunz et al. (2003), Frobenius et al. (2003), and Dular et al. (2003, 2006a) have performed three-dimensional simulations. Figure 5.4 shows a good agreement between the computed cavity shape and experimental observation for a three-dimensional hydrofoil, as computed by Frobenius et al. (2003).

Many researchers have also applied multiphase flow cavitation models to studies on instabilities of cavitating flows. Leroux et al. (2003) and Coutier-Delgosha et al. (2003c) performed two-dimensional unsteady simulations of the cavitating flow over a hydrofoil section using the barotropic-state-law model, and they reported good predictions of the frequencies of the cavity oscillation. Coutier-Delgosha et al. (2003b), Iga et al. (2003), Iga et al. (2004), and Leroux et al. (2005) obtained similar results.

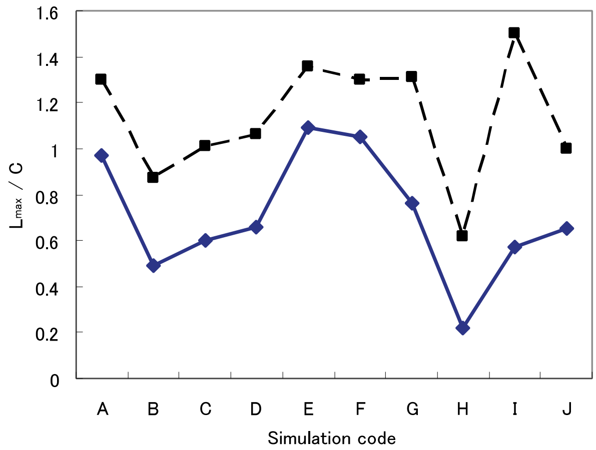

Figure 5.3 Comparison of the computed maximum cavity lengths over the CAV2003 hydrofoil at two cavitation numbers (where σ = 0.8 are the blue diamonds and σ = 0.4 are the black squares).

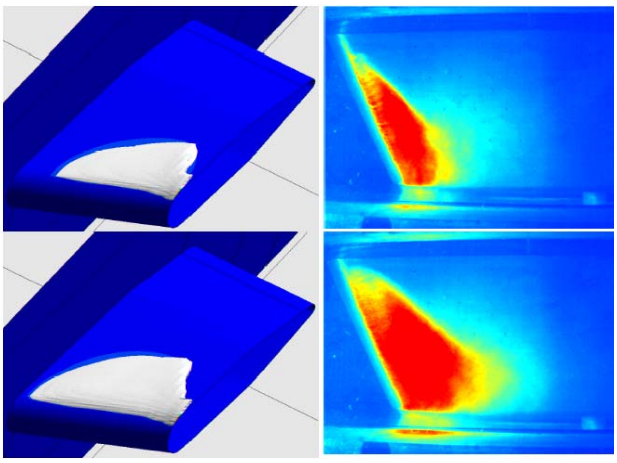

Figure 5.4 Comparison of the cavity shapes between experimental observations and simulations by Frobenius et al. (2003).

<u>Application to Engineering Flows, Pumps, and Propellers.</u> Multiphase flow cavitation models have also been applied to flows of engineering interest such as flows in a pump or

through a marine propeller. Yamada et al. (2003), Nohmi et al (2003), Okita et al. (2003), Kimura et al. (2006), Hosangadi et al. (2006), and Flores (2006) have applied these models extensively to pumps. Bakir et al. (2003) and Ait-Bouziad et al. (2003) simulated cavitation in a pump inducer using commercial CFD software with multiphase flow modeling. Their results are in good overall agreement with experimental results with respect to the head drop, the size and location of the cavity, and the inception. However, Bakir et al. (2003) stated that the simulation under-predicted the head drop at high flow rate and that the cavitation model itself requires careful testing for the determination of empirical constants. Fukaya et al. (2003) applied a bubble-flow-type multiphase flow model to cavitating flow in an axial-flow pump. Although the predicted cavitation performance was only in qualitative agreement with the measurements, they refer to the potential of predicting impulsive pressure due to the collapse of bubbles.

Streckwall and Salvatore (2007) compared the results of RANS codes with multiphase flow models from various laboratories predicting propeller performance and cavitation in uniform flow. While the thrust and torque predictions were close, the cavity patterns showed some differences, as seen in Figure 5.5. A surprising result was that the surface pressures under the cavity were not constant in some of the codes.

Watanabe et al. (2003) and Rhee et al. (2005) simulated cavitating flow through a marine propeller using commercial software, and they showed that the predicted cavity shape agrees with experimental results. Kawamura et al. (2006) presented an unsteady simulation of cavitation on a marine propeller operating in a non-uniform wake. The time-dependent growth and collapse of the sheet cavity in the wake is reproduced, as shown in Figure 5.6. This capability is necessary for predicting the pressure fluctuation at the blade frequency.

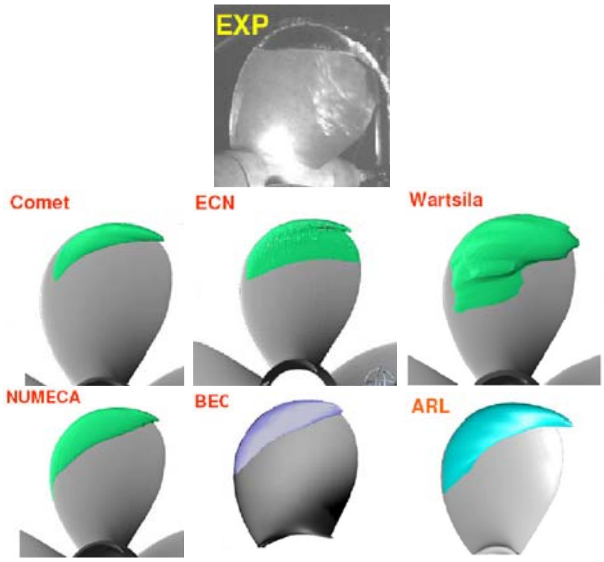

Figure 5.5 Comparison of measured and computed cavity patterns (vapor volume fraction c_V=0.5)—as reported by Streckwall and Salvatore (2007).

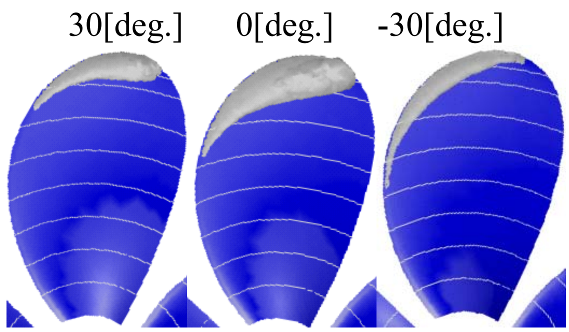

(a) Calculation

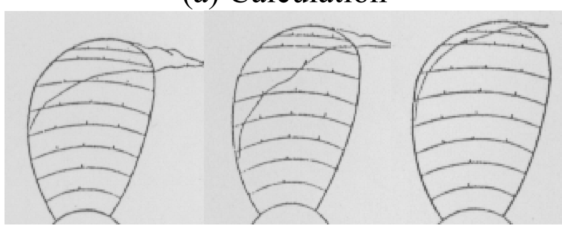

(b) Experiment

Figure 5.6 Comparison of the unsteady cavity patterns in the (a) experiment and (b) calculation given by Kawamura et al. (2006).

Prediction of Cavitation Inception. Prediction of cavitation inception is also very important from an engineering point of view. However, most multiphase flow cavitation models use the assumption that the growth and collapse of cavitation bubbles occur in a very short time. This assumption may be valid for predicting the inception of attached sheet cavitation, but it is probably inappropriate for inception of traveling bubble cavitation or vortex cavitation. Therefore, several researchers have applied more complex bubble dynamics models to the prediction of inception in vortices. Hsiao and Chahine (2004) applied spherical and non-spherical bubble dynamics models to the prediction of tip-vortex cavitation of a finite-span hydrofoil, and they showed that non-spherical bubble deformation is important for the accurate prediction of cavitation inception.

Kim et al. (2006) studied the inception of tip-leakage cavitation within a ducted propeller, and Wienken et al. (2006) have studied the inception in the flow past a square cylinder. Kim et al. (2006) used a locally-refined grid around the tip for resolving the vortex core, while Wienken et al. (2006) applied LES to capture the unsteady vortices.

<u>Prediction of Cavitation-Induced Pressure Fluctuations.</u> Occurrence of unsteady cavitation can induce significant pressure fluctuations on the surrounding structures. These pressure fluctuations are particularly important in the design of the propulsion system for a ship. While there are relatively many papers on the prediction of the influence of cavitation on hydrodynamic performance, publications of these pressure fluctuation have been very limited.

Very recently, Kawamura and Kiyokawa (2008) simulated cavitating flow around a propeller rotating in a wake of a ship using the approach used by Kawamura et al. (2006). Figure 5.7 shows the predicted hull surface pressure fluctuation at the blade frequency. It is shown that the magnitude and extent of the pressure fluctuations are greatly increased with the occurrence of cavitation. However, the detailed comparison shown in Figure 5.8 indicates that the pressure fluctuation associated with cavitation is still under-predicted by the simulation. Kawamura and Kiyokawa (2008) also pointed out that the higher-frequency components are not reproduced in the simulation.

Although more extended validation is desired, this study suggests that multiphase flow modeling has the potential ability to predict cavitation-induced pressure fluctuations, at least at low frequencies.

<u>Prediction of Cavitation Erosion.</u> The prediction of erosion due to cavitation is considered very difficult because micro-scale bubble dynamics play an important role. Fukaya et al. (2006) attempted to predict the cavitation erosion on a centrifugal pump blade using a multiphase flow cavitation model based on detailed bubble dynamics. They defined *cavitation intensity* as the frequency of the bubble collapse events in the simulation, and they related it with the erosion. Figure 5.9 shows the comparison between the predicted cavitation intensity and the result of a paint test.

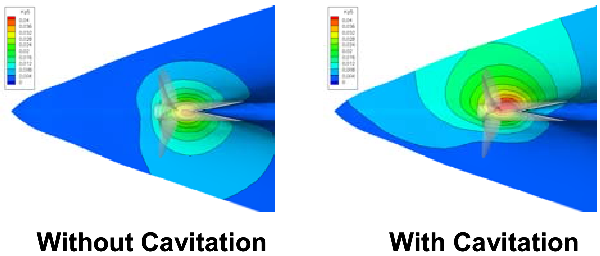

Figure 5.7 Magnitude of the pressure fluctuations on the hull surface at the blade frequency, as predicted from a RANS simulations by Kawamura and Kiyokawa (2008).

Dular et al. (2006b) have experimentally shown that the standard deviation of the void fraction can be correlated with the cavitation damage, and they applied this correlation to the prediction of erosion by CFD. Although the agreement between the prediction and the experiment in these two studies is not very satisfactory, the two approaches seem to be effective, and one can expect improvements in the future.

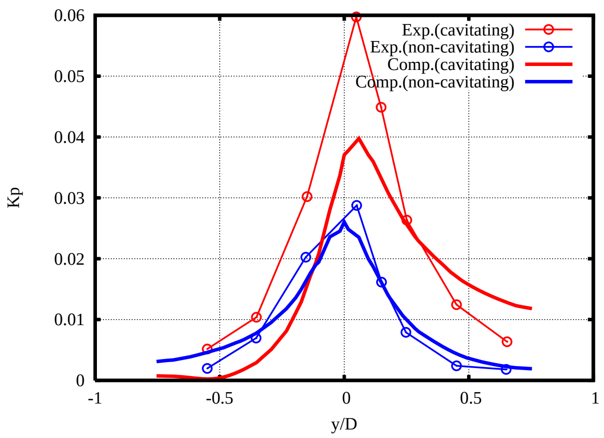

Figure 5.8 Comparison of the measured and computed hull surface pressure fluctuations at the blade frequency, as given by Kawamura and Kiyokawa (2008).

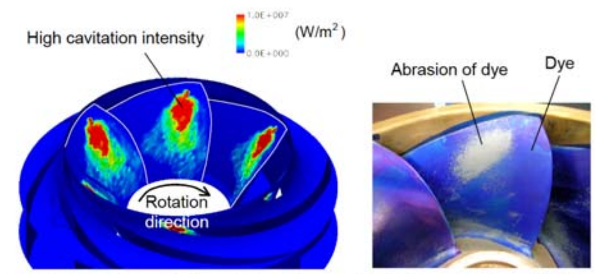

(a) Predicted cavitation intensity (b) Visualized cavitation erosion area

Figure 5.9 Predicted *cavitation intensity* and comparison with the result of an experimental paint test, as given by Fukaya et al. (2006).

Prediction of Cavitation Thrust Breakdown. One of the most detrimental effects of cavitation within a propulsor or pump involves the performance breakdown of thrust, torque, and total-head rise. Recently, several investigators have begun to show some promising numerical simulations of cavitation breakdown for pumps and propellers based on three-dimensional RANS solvers with multiphase flow models.

To evaluate the three-dimensional, quasi-steady cavitation within three different pumps, Coutier-Delgosha et al. (2002) used a commercial RANS code, which they adapted to account for the cavitation phenomenon. They described the cavitating flow as a single fluid model—with a barotropic law that links the local density with the local static pressure. Their simulations of cavitation breakdown quantitatively compared well with experimental data for two radial-flow (or centrifugal) pumps. However, while they obtained good qualitative agreement; they did not obtain accurate quantitative agreement with experimental data for a turbopump inducer.

Dupont and Casartelli (2002) described several approaches for modeling cavitation with three-dimensional RANS simulations, and they used two different approaches to predict the cavitation in two centrifugal pump impellers—impellers with the same specific speed, but with small geometrical differences that lead to significant differences in cavitation development. First, they used a commercial RANS code, which has a cavitation module using a coupled approach. Then, using a non-coupled approach, they used their own RANS code to compute the non-cavitating pressure distribution, which they used to simply solve the Rayleigh-Plesset equation for computing the cavity shapes. They developed this simple method and calibrated it using test data as an alternative to the expensive coupled approach—but they realized its physical limitations, especially if the cavities begin to detach. Nonetheless, they obtained comparable agreement between the two approaches in predicting the cavity shapes and the 3% drop in total head that marks the point of cavitation breakdown—with both approaches giving fair comparisons with experimental results.

For the cavitating flow through a centrifugal pump impeller, Frobenius et al. (2002) performed both an experimental investigation and a numerical investigation, using their own developed RANS code with a cavitation model based on bubble dynamics. They used a one-fluid model, which they treated as a homogeneous bubble-liquid mixture. Their method included a transport equation for the vapor fraction and the Rayleigh-Plesset equation to model bubble growth and collapse. For the total-head drop associated with cavitation breakdown, they showed good agreement between their experimental and numerical results. At the point of incipient cavitation, they also showed good agreement with blade pressure distributions. However, with decreasing cavitation number, they showed less favorable agreements for both blade pressure distributions and void fraction distributions.

Using their own developed code, Lindau et al. (2005) performed a simulation of propeller cavitation thrust breakdown based on a homogeneous, multiphase RANS formulation. They treated both the liquid and vapor phases within each control volume and discretely modeled the mass transfer between phases, a multiple species transfer model of multiphase flow that they felt offers a more flexible physical approach. For this propeller test case, they predicted the critical cavitation number leading to thrust and torque breakdown, providing good agreement with experimental data over a wide range of flow coefficients.

5.3 Cavitation Predictions using LES and DES

For the simulation of turbulent flows of practical interest, most organizations currently use solvers of the Reynolds-averaged Navier-Stokes (RANS) equations. This choice holds for cavitating flows as well as non-cavitating flows. RANS solvers are based on time- or ensemble-averaging of the Navier-Stokes equations. The averaged velocities and pressures are explicitly solved, while the apparent Reynolds stresses are modeled using a turbulence model. For practical problems, two-equation models—such as k-ε, k-ω, or q-ω models—or one-equation models—such as the model developed by Spalart and Allmaras (1994) —are usually applied. Because only the averaged quantities are explicitly solved, the required computational load is usually moderate. However, it is known that the quality of the turbulence model is not always sufficient, especially in regions of strong adverse pressure gradients, flow separation, and flow rotation.

In recent years, organizations have shown an increased interest in large eddy simulation (LES). In contrast to simulations using the RANS equations, LES is based on spatial filtering, so that filtered variables are functions of space and time. LES resolves the largest turbulent eddies and only requires modeling of eddies smaller than the grid scale. Thus, a greater grid resolution gives a greater resolution on the turbulence. Consequently, careful LES requires much denser grids than RANS—and, hence, much more computational effort and a much larger quantity of computation data.

Given the significant increase in computational effort between RANS simulations and LES, researchers have developed detached eddy simulation (DES) to reduce the computational effort of LES, but still resolve the important turbulent structures. In fact, one could describe DES as a mix of RANS and LES. One models the near-wall flow (or boundary layers) with RANS and the outer flow (and corresponding detached eddies) with LES. The change from RANS to LES is governed by a comparison of a local grid scale and a suitable turbulence length scale. One issue still involves how to make the transition from the RANS domain, with its averaged turbulent quantities, to the LES domain—which requires much more detailed turbulent information.

Cavitation modeling within RANS, DES, or LES is based on the same approach—assuming a continuum mixture fluid and solving an additional transport equation for a void fraction with appropriate source terms. However, in DES or LES, local and instantaneous pressure fields are better resolved than in RANS, possibly leading to significant improvements in the prediction of cavitating flows.

Within the literature review of recent research on multiphase flow modeling, the committee has given several examples of using LES and DES. These efforts included the work by Wienken et al. (2006), Wosnik and Arndt (2006), Persson et al. (2006), and Wang and Ostoja-Starzewski (2007).

Rhee et al. (2007) discussed new commercial RANS/LES hybrid schemes, which are based on a homogeneous mixture using a single set of momentum and turbulence equations.

The method uses the reduced Rayleigh-Plesset equations to account for phase changes, including non-condensable gas and pressure fluctuations. Slip is allowed between phases, and the phase change model can be user-defined to include mass source terms. Rhee et al. (2007) gave example calculations that compare open-water propeller test data, in a fully-wetted condition and with extensive tip vortex cavitation conditions. They showed good agreement of the values for thrust coefficient, K_T, and torque coefficient, K_Q.

For cavitation inception within a circular jet flow, Edge (2007) computed this complex vortical flow field with a single-phase DES. Then, he released cavitation nuclei into the jet flow and computed the radial growth of the nuclei using a code that solves the Rayleigh-Plesset equation, with the dispersion of the bubbles governed by a semi-empirical equation of motion. This uncoupled methodology proved very useful in evaluating parameters that determine jet cavitation inception—such as the size and characteristics of the jet and the initial nuclei size. The primary objective of this research was to develop a scaling relationship for cavitation inception.

Huuva (2008) applied LES and DES to cavitating flow over a NACA0015 foil with a flat tip and over a Twist11 hydrofoil. He indicated that LES and DES computations resolve the structure of cavitating flows in more detail compared with RANS computations, and that this added detail can cause significant qualitative difference in the collapsing behavior of cavity over hydrofoils. Meanwhile, he also mentioned that RANS computations are sufficiently reliable in the prediction of basic quantities such as cavity volume or shedding frequency.

6 RUDDER CAVITATION

Problems of rudder cavitation erosion had been somewhat out of focus in the shipbuilding industry in the 1970's—since, at that time, ships were sailing quite slow due to high oil prices. Even with oil prices high again, ships—especially container vessels, roll-on/roll-off (RoRo) ferries, and liquefied natural gas (LNG) carriers—tend to sail at high speed. Consequently, prevention of rudder damage due to cavitation has become an issue again.

Billet et al. (2005) and the Specialist Committee on Cavitation Erosion on Propellers and Appendages on High Powered/High Speed Ships for the 24th ITTC addressed the topic of cavitation damage on *conventional* rudders. They concluded that the propeller(s) and rudder(s) —and any other appendages—must be designed as a unit, with careful attention paid to both the hydrodynamics and the materials. They also stressed the importance of off-design operating conditions. Finally, they recommended more documentation of the observed full-scale erosion patterns—not only to improve correlations of model-scale tests, but also for improvement of the design methodology to reduce potential cavitation erosion.

Figure 6.1, taken from Friesch (2006), shows the typical areas of rudder erosion damages on a conventional semi-spade rudder. Cases have been reported, where serious rudder repair work had become necessary long before the regular five-year service interval was completed. The cavitation phenomena responsible for damage in Figure 6.1 include gap cavitation in both the vertical gaps (Zones B and C) and horizontal gaps (Zone D), sheet or cloud cavitation in thickened geometry regions such as around the pintle area (Zone A), and vortex cavitation at the rudder sole (Zone E).

The 25th ITTC Specialist Committee on Cavitation will extend the recommendations of this previous ITTC committee by addressing the methods for predicting cavitation and erosion damage on unconventional rudders or on rudders behind highly-loaded propellers. For clarification, the committee will address two fundamental questions in Appendix A: "What is an unconventional rudder?" and "What is a highly-loaded propeller?"

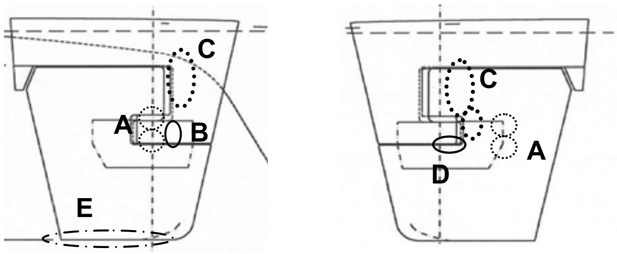

Figure 6.1 Critical areas of cavitation damage on a conventional semi-spade rudder as described by Friesch (2006).

As a consequence of the issues addressed in Appendix A, the recommendations in Sections 6.2 and 6.3 for rudder cavitation tests should be applied whenever the ship does not have a conventional symmetric semi-spade or spade rudder, or whenever the ship has a propeller power density of more than 800 kW/m^2. It might be pointed out that all of the large and fast container ships of today, which are known to be highly susceptible to rudder cavitation erosion, fall into this category, since they typically have a propeller power density greater than 1,000 kW/m^2.

6.1 Rudder Erosion Issues

Of course, all rudder erosion problems mentioned by the previous ITTC Specialist Committee on Cavitation for conventional rudders also apply for unconventional rudders. Additional problems arise from the much more complex geometry of unconventional rudders. They have more gaps and/or more sharp edges, as illustrated in the figures in Appendix A. Sharp edges always imply high flow velocities, or low static pressures. The consequence is an increasing risk of cavitation. The same holds for a flow that accelerates through a narrow gap.

The problems involved in a rudder behind a highly-loaded propeller have already been addressed in the previous section. The high propeller loading increases not only the axial inflow velocity to the rudder, but also the non-uniformity of the inflow due to the increased swirl in the propeller slipstream. Adaptation of the rudder to this non-uniformity requires non-uniformity of its geometry, which again results in either sharp edges or edges with small radii—as shown, for instance, in Figures A.5 or A.8.

Issues also arise during cavitation performance testing on models of unconventional rudders or rudders behind highly-loaded propellers, especially from cavitation within the gaps and from the propeller vortex cavitation impacting the rudder. Gap flow is influenced by the boundary layer thickness upstream and within the gap. Because the Reynolds number is smaller in a model test, the boundary layer is thicker, which hinders the gap flow unrealistically. Consequently, the gap flow is slower at model scale and the cavitation inception is delayed.

Regarding the impact from the propeller, its hub and tip vortex cavitation need to be mentioned. Both cavitating vortices are known to be possible sources of erosion when impacting the rudder. The existence of these vortices is unavoidable according to the first Helmholtz theorem. Their strength correlates with the loading of the propeller—which makes them critical, especially with highly-loaded propellers. In this case, these hub and tip vortices may be strong enough to generate cavitation within their core, and their stability might be great enough to remain cavitating until they have reached the rudder. In general, these kinds of vortex cavitation do not cause any erosion problem at the propeller, because they appear downstream of the propeller. But, they may damage the rudder, especially when collapsing on the rudder surface.

At least since the fundamental work of McCormick (1962), it is known that vortex cavitation inception depends on the Reynolds number—that is, it appears later and weaker at model scale. This Reynolds number dependency is because the rotational flow in the vortex core is weakened by the exaggerated viscosity at model scale. As a consequence, rudder erosion due to propeller vortex impact might be under-predicted from model tests.

6.2 Experimental Methods for Rudder Cavitation Prediction

As mentioned previously, not many organizations from the worldwide cavitation community responded to the rudder cavitation portion of the committee's survey—and, the few organizations that did respond, did not elaborate on the experimental methods. Nonetheless, with the difficulty in modeling cavitation erosion, experimental methods still offer the best means of assessing rudder cavitation.

Scale Effects. Even more importantly than for model tests of propeller cavitation, one must account for scale effects when conducting model tests to investigate rudder cavitation. This situation is especially true for unconventional rudders. In this respect, the result of the survey was very clear. Most organizations with full-scale ship experience answered that almost all rudder cavitation phenomena (gap, sheet, and/or vortex cavitation), as well as the range of rudder angles where they occur, are under-predicted from a model test. Just a few organizations consider these values as similar, and no organization answered that these phenomena are over-predicted.

For a normal cavitation test, one places the rudder behind a propeller, and a K_T-identity exists between model and full scale. Then, the ratio between model- and full-scale Reynolds numbers is the same for the propeller and for the rudder. Nevertheless, the absolute value of the Reynolds number locally at the rudder is typically only 50% of the model propeller Reynolds number. Even if this value is well above the critical value of $Re > 300{,}000$ (which is known to be sufficient for a propeller), the Reynolds number may still be insufficient to guarantee fully turbulent flow over the rudder.

Regarding gap cavitation, scale effects also include the viscosity effect within those gaps. Thus, the resulting boundary layers are too thick at model scale, hindering the flow through the rudder gaps—and, in this way, certainly delaying gap cavitation. Such a delay has been reported by 86% of the organizations having full-scale experience (as estimated from the survey).

As mentioned previously for propeller vortex cavitation, model-scale rudder vortex cavitation may also suffer from scale effects caused by the Reynolds numbers being too low during testing. McCormick (1962) performed a fundamental investigation and developed a well-known equation for the inception of vortex cavitation,

$$\left(\frac{\sigma_{i,\,full\ scale}}{\sigma_{i,model\ scale}}\right)=\left(\frac{\mathrm{Re}_{full\ scale}}{\mathrm{Re}_{model\ scale}}\right)^{m}, \qquad (6.1)$$

which he originally developed for delta wing forms. Several researchers suggested various values for the exponent, m, depending on arrangements and conditions. The most recent approach is reported by Bulten and Oprea (2006). Anyway, rudder cavitation is normally investigated to predict erosion problems at full scale. While the equation developed by McCormick (1962) and others may be applicable for the inception of rudder vortex cavitation, it does not help investigators to scale the erosiveness of developed vortex cavitation.

Assessment of Cavitation Erosion. The biggest problem with respect to model-test-based predictions of rudder cavitation erosion is the actual assessment of the cavitation at model scale. Propeller cavitation observed in stroboscopic light has been correlated to full-scale propeller erosion damage for more than a hundred years. Even if the fundamental physical mechanism is still not clear, this experience represents a sufficient basis for assessment. The lack of such experience is one of the problems involved in high-speed video observations of cavitation at model scale. Cavitation simply looks different using this tool and experience needs to be acquired to judge it. The same holds for rudder cavitation, even under conventional recording conditions: phenomena such as stable sheet cavitation, which are known to be non-critical for propellers, seem to be erosive on a rudder surface. Gap cavitation phenomena never occurred on a propeller (except very locally behind the palm of controllable pitch propellers). So what does erosive gap cavitation look like? How does one distinguish between erosive and non-erosive rudder sheet cavitation?

One important, but time-consuming, approach to overcome this problem in the future is to gather the missing experience by performance of frequent full-scale rudder cavitation observations. Miller and Wilczynski (2006) have recently published such a correlation study. Also, Friesch (2006) gave an excellent overview of this issue. An alternative, but not a very satisfying, approach is the use of soft-ink testing methods for erosion assessment. Here, to achieve better reliability, one must follow approved standard procedures as established for propeller erosion tests by the EROCAV project and reported by Billet et al. (2005) and the Specialist Committee on Cavitation Erosion for the 24th ITTC.

Recommendations for Unconventional Rudder Cavitation Tests. Following the previous sections, the committee has developed recommendations for model testing of unconventional rudders or rudders behind highly-loaded propellers:

(1) The recommendations given by Jessup et al. (2002) and the Propulsion Committee of the 23rd ITTC regarding cavitation testing at model scale in general apply to the tests for unconventional rudders as well. The operation of the complete unit of rudder *and* propeller in most realistic propeller inflow conditions is essential for unconventional rudders as well. Use of complete ship models for wake generation should be considered wherever possible.

(2) For unconventional rudders, the exact reproduction of the complex rudder geometry is essential. Sharp edges at full scale need to be modeled sharply. Penetrating gaps at full scale need to be modeled as such to allow water passing through the gap. Mechanisms of flap rudders, for example, need to be modeled.

(3) The local Reynolds number at the rudder profile should be greater than 300,000 to avoid laminar flow effects.

(4) As long as nothing better is known (refer to the following recommendations for future investigations), one should investigate a much wider range of rudder angles than has to be guaranteed for erosion-free operation at full scale. If a model rudder suffers from erosive gap cavitation at a 5° rudder angle, for example, it might show this phenomenon at full scale for a 3° rudder angle. Bear this in mind!

(5) Larger-scale part models may be used to test local gap cavitation phenomena or cavitation phenomena occurring at rudder details like spoilers. Whenever such part models are tested in uniform inflow, a calibration is needed based on knowledge of the cavitation phenomena occurring at full scale for those rudder details: the test conditions (tunnel pressure, flow speed, and rudder angle) need to be modified until the phenomenon to be investigated occurs as at full scale. Then, geometric modifications can be investigated keeping those test conditions constant. Without such a calibration, the reliability of a part-model rudder cavitation test is regarded as poor.

Requirements for Future Investigations. While the previous recommendations should be followed under present conditions, future investigations can certainly improve model-scale cavitation testing for unconventional rudders or rudders behind highly-loaded propellers. Here, the committee provides some suggestions:

(1) The application of rudder leading-edge roughness should be considered to further reduce laminar flow effects in this area.

(2) Intentional widening of gaps (that is, local deviation from geometric scaling) should be investigated as a means to compensate for the overly thick boundary layers within gaps during most model-scale tests.

(3) Full-scale rudder cavitation observations and corresponding monitoring of rudder

erosion damages are necessary to gather experience for visual assessment of rudder cavitation at model scale.

(4) The previous requirement for full-scale rudder cavitation observation especially applies for high-speed video observations.

(5) Improvement of the soft-ink method is required to improve its reliability and to overcome the necessity of visual assessment of erosiveness. Model basins need to introduce their own standard procedures—individually adjusted to their rudder materials, coatings, and standard test procedures.

6.3 Numerical Methods for Rudder Cavitation Prediction

In spite of much effort, hydrodynamic researchers have yet to develop a universally-accepted numerical method to predict the cavitation erosion—largely because the physical mechanism of the erosion is not fully clarified. Only a few researchers have reported their studies since the last ITTC.

Hence, in practice, to evaluate the possibility of the occurrence of cavitation erosion, designers of rudders, without model tests, must use indirect information—such as the pressure distribution on the rudder surface obtained from numerical methods or the empirical approaches based on the designer's experience. These numerical methods can be divided into the potential-flow and viscous-flow approaches.

The potential-flow approach—such as a lifting-surface or a boundary-element method (BEM)—is traditionally used in propeller and wing design, and it can provide information on the cavitation occurrence on the blade surface of the rudder. Especially for the rudder located just behind a propeller, the significant interaction between the propeller and the rudder can be considered by using the same numerical methodology. Of course, the calculation for the rudder alone with the appropriate inflow is possible. BEM codes give more realistic results than the lifting-surface theory, because the rudder is relatively thicker than the propeller blades.

In general, the potential-flow approach requires low computational costs—and, additionally, the performances of the propeller as well as the rudder can be predicted simultaneously. Hence, this approach is still widely used, especially during the initial design stage.

However, drawbacks exist in the potential-flow approach, since the tip vortex induced by the thick bottom edge of the rudder is not simulated precisely, and the viscous effect is neglected. As a result, potential-flow methods cannot predict the vortex cavitation around the bottom edge, without specific additional modeling. Also, for the semi-spade rudder, it is impossible to represent the gap between the rudder blade and the horn using the potential-flow approach. Reasons for this difficulty are that the flow pattern and pressure distribution around the gap are quite complex—including the flow separation and vortex generation—and are highly affected by small changes and viscous effects in the gap geometry.

Recently, with advances in computer technology, designers have increased their use of viscous-flow solvers, with the exact shape of the rudder geometry. In this approach, both single-phase flow solvers and multiphase flow solvers exist—as reported previously in this report. The single-phase flow calculation predicts the flow pattern and pressure distribution around the rudder, which gives an indication of cavitation inception wherever the local static pressure falls below the vapor pressure. As discussed previously in this report, a multiphase flow calculation gives information on the unsteady behavior of developed cavitation. However, in practice, few designers actually use multiphase flow calculations, because of high computational costs and the lack of universal acceptance of the cavitation-erosion models.

Under these circumstances, another major factor that affects the reliability of the numerical results for the rudder is how to consider the propeller action. The simple way is to assume the inflow and to calculate the flow around the rudder alone. The assumption of the inflow can be based on measurements in a model test or on computations of the propeller. Of course, this method does not include the interaction between the propeller and the rudder.

Conversely, one could compute the flow around the propeller and rudder simultaneously. However, this method increases the computational costs, and it must correctly model the interface between the rotating computational grid in the vicinity of the propeller and the stationary computational grid in the vicinity of the rudder. A sliding mesh, with proper interpolation, is one example of modeling this interface.

Alternatively, one could simplify the propeller as a momentum disk and treat the thrust and torque of the propeller as momentum sources—iteratively determined by the potential-flow codes for the propeller in general. Hence, performance of the rudder and propeller is predicted with a low computational cost. However, this method has problems in properly capturing the tip and hub vortices generated from the propeller.

7 WATERJET CAVITATION

Waterjets have become the standard propulsion system for surface vessels with cruising speeds greater than about 25 knots, where waterjets can become more efficient than the propellers fit for those vessels—especially for vessels with draught restrictions that limit the propeller diameter. Compared to vessels using propellers, vessels using waterjets have the advantage of higher speed operation without thrust breakdown from cavitation, especially for speeds greater than 30-35 knots. Even at lower speeds, vessels with shallow-water requirements may also employ waterjets. Furthermore, when installed with steerable nozzles, waterjets offer greater maneuverability. Also to their advantage, waterjets absorb power from the main engine almost independently of ship speed. Therefore, standard waterjet units have the ability to operate over a large speed range without placing undue stress on the transmission and engine.

Since the ITTC has never focused on waterjet cavitation issues, the 25th ITTC Specialist Committee on Cavitation will provide a fairly detailed introduction to these issues in Appendix B. The rest of this section will focus on the modeling and scaling of waterjet cavitation.

7.1 Modeling of Waterjet Cavitation

Traditionally, most modeling of waterjet cavitation has involved experimental testing. As mentioned previously, the ITTC has developed procedures for the determination of the powering characteristics of waterjet-propelled vessels, and Hoyt et al. (1999) and the Specialist Committee on Waterjets for the 22nd ITTC recommended self-propulsion tests, waterjet system tests, and pump tests. In this section, the committee will comment on the usefulness of these three types of waterjet tests for determining the cavitation performance. In addition, the committee will focus much of the discussion on how recent advances in CFD can address the modeling of waterjet cavitation.

Self-Propulsion Tests. Similar to self-propulsion tests for vessels powered by propellers, self-propulsion tests for vessels powered by waterjets involve models tested in a towing tank. To measure the model-scale resistance, waterjet testing requires that one conceal the inlets with an appropriately-contoured cover. For waterjet-powered tests, Hoyt et al. (1999) have recommended many additional measurements than one would use for propeller-powered tests. Essentially, these measurements allow one to determine the momentum flux and energy flux at several key stations from upstream of the waterjet through the pump and into the downstream jet.

Self-propulsion tests are not appropriate for the evaluation of cavitation. Most facilities used for self-propulsion tests cannot be depressurized—so, one cannot achieve cavitation similarity. Even when it is possible to achieve cavitation similarity, cavitation viewing is difficult in the inlet region and almost impossible in the pump region. For well-designed inlets, cavitation should only be an issue at off-design values of the inlet velocity ratio, *IVR*, (as defined in Appendix B) so one would have to attempt to view the cavitation at the appropriate values of *IVR*. Furthermore, operation at an appropriate Reynolds number is necessary for cavitation testing. For instance, characteristics of a cavitating flow field, such as flow separation, depend on the Reynolds number. The speed of the towing-tank carriage and the small dimensions of the waterjet model do not allow for testing at an appropriate Reynolds number. In most cases, the waterjet pump used for self-propulsion tests is not even a scaled model of the actual waterjet pump; it is simply a surrogate pump that ingests the appropriate mass flow rate.

<u>Waterjet System Tests.</u> Waterjet system tests involve either closed-loop or open-loop experiments of an actual waterjet inlet and pump, without an actual model of the ship hull. While some waterjet system tests involve a uniform inflow, more appropriate tests should incorporate incoming boundary layers—which are ingested through the inlet—that properly represent the hull boundary layer. As pointed out by Hoyt et al. (1999), these tests can address cavitation observations of the inlet lip and ramp, as well as observations of pump cavitation.

<u>Pump Tests.</u> If one does not have an appropriate setup to conduct a waterjet system test and if the self-propulsion test is at too small of a Reynolds number or uses a surrogate pump, then historically waterjet designers have relied on tests within a pump loop. One valuable characteristic of pump-loop testing is the ability to change the resistance of the pump loop and operate the pump at a large range of flow coefficients, allowing the designer to evaluate the off-design characteristics of the pump—from stall at low flow coefficients through the design flow coefficient through high flow coefficients, where lower values of static pressure could enhance issues related to cavitation. Fortunately, most waterjets tend to operate at a nearly constant flow coefficient. However, if this operational flow coefficient differs significantly from the design coefficient, this off-design testing can prove useful.

Hoyt et al. (1999) also feel that pump tests can address how cavitation affects waterjet performance, particularly in evaluating cavitation thrust breakdown. Control of the static pressure within the pump loop allows for testing at different cavitation numbers. The cavitation number corresponding to a 3% decrease in total-head rise across the pump is commonly used to identify the point of cavitation breakdown. In most pump tests, the pump inflow comes from flow through a pipe or through a bellmouth nozzle, which does not represent the inflow that the pump will ingest within an operational waterjet propulsion system. One could attempt to better model the correct inflow by using properly-designed honeycomb, screens, fins, and/or pipe elbow. In any event, the testing should include a measurement of the pump inflow.

<u>Computational Fluid Dynamics.</u> While numerical modeling of cavitation phenomena has existed for many years, the complexity of waterjet systems—for both the physics of the flow fields and the geometry—has historically led organizations to rely on experimental modeling. However, improvements in computational tools and computer power—as well as the high cost and time required for experimental modeling—have recently led organizations to rely more and more on numerical modeling to address cavitation behavior in waterjets. The literature reviews in Appendix B certainly reflect the increased use of CFD. And, as reported in previous sections of this report, even more powerful CFD tools are becoming available to investigate waterjet cavitation issues.

For cavitation inception, where the volume of the cavitation is a very small percentage of the flow field, one can suitably assume that the existence of the cavitation will have a negligible impact on the flow. Therefore, one can numerically model the bulk flow field and then use that simulation as input to numerically model the bubble dynamics, if desired. The simulation of the bubble dynamics will not influence the simulation of the bulk flow field.

Numerical analysts have had success in modeling surface (sheet) cavitation inception by solving the RANS equations. Following the proper use of the RANS solver—such as using adequate grid quality—the minimum static-pressure region near a solid surface will correspond closely with the region of surface cavitation inception. While unsteady flow phenomena can alter this result, these types of simulations have matched well with experimental results for visual observation of inception.

While RANS simulations have proven successful in determining the minimum static-pressure region near a surface, they have not been very successful in determining the minimum static-pressure region within a vortex core. Obtaining adequate grid resolution within the vortex core is certainly one problem, but the effects of unsteady flow phenomena are an even greater problem, including unsteadiness due to turbulent-flow structures. Traditional turbulence modeling within a RANS solver *averages out* the unsteadiness of these turbulent-flow structures. Therefore, numerical modeling of vortex cavitation inception requires a direct simulation of the larger, energy-containing turbulent scales. LES has become a more mature method to model these important turbulent scales, but the computational costs remain prohibitively large. However, methods like DES allow one to compute these important turbulent scales only in the areas of interest, reverting to a RANS simulation elsewhere. These types of methods are beginning to make the numerical modeling of vortex cavitation inception possible, but they still remain primarily a research topic.

The most detrimental effect of cavitation within a waterjet involves the breakdown of pump performance parameters such as thrust, torque, and total-head rise. Recent investigations have led to the development of multiphase flow models using three-dimensional RANS solvers that have shown some promising numerical simulations of cavitation breakdown for pumps and propellers. Multiphase flow modelling is further advanced for cavitation breakdown, since it is a more global cavitation event, not a local event such as cavitation erosion. These methods should be utilized in future modeling of cavitation breakdown in waterjet pumps.

The prediction of erosion due to cavitation is very difficult because micro-scale bubble dynamics play an important role. Therefore, numerically modeling the behaviour of cavitation erosion is a research topic in its infancy. Researchers have pursued two approaches to this multiphase flow modeling problem. The first approach uses a cavitation model that includes modeling of the micro-scale bubble dynamics, which estimates the impulsive pressure directly. The second approach models the relationship between the fluctuation of the void fraction and the occurrence of erosion. To date, both approaches have predicted erosion areas that qualitatively agree with experimental data, but much further research is required to achieve quantitative predictions, especially for the complex geometry and flow fields found in a waterjet pump.

7.2 Scaling of Waterjet Cavitation

As discussed previously, and in Appendix B, one attempts to quantify or categorize cavitation performance using the cavitation number (or some related parameter). When using experimental modeling to determine the behaviour of cavitation in a waterjet, test facilities usually dictate the use of model-scale hardware. Unfortunately, the cavitation number that characterizes a cavitation phenomenon at model scale may differ for the full-scale prototype hardware. These differences result from cavitation-scale effects—such as the method of cavitation detection (visual or acoustic) and water quality, as describe in depth by Billet et al. (2002) and the Specialist Committee on Water Quality and Cavitation for the 23rd ITTC.

Other cavitation-scale effects can include Reynolds-number effects, geometry effects (such as surface roughness or manufacturing tolerances), turbulence, and the residence time that nucleation sources spend within low-pressure regions of the flow.

The scaling of cavitation inception depends strongly on whether one is concerned with surface (sheet) cavitation inception or vortex cavitation inception. For experimental models with geometric similarity, one is usually not able to run the model-scale test at the full-scale Reynolds number. However, for surface (sheet) cavitation inception, after one accounts for water-quality effects, Reynolds-number effects may be small and are usually neglected. The exception can be for the Reynolds-number effects on flow separation, which can influence cavitation on a waterjet inlet. However, for a waterjet inlet, dynamic similitude of the incoming boundary layer is probably more important than Reynolds-number effects. The biggest problem is that modeling the highly unsteady, three-dimensional boundary layer that a full-scale waterjet ingests at sea is probably impossible in a model-scale test facility. For the waterjet pump, cavitation inception probably occurs in the tip-leakage vortex rather than on the rotor-blade surface, so the Reynolds-number effects on surface cavitation may not be of primary importance anyway.

For vortex cavitation inception, one traditionally scales the inception cavitation number using some form of the equation presented by McCormick (1962),

$$\left(\frac{\sigma_{i,full\ scale}}{\sigma_{i,model\ scale}}\right)=\left(\frac{\mathrm{Re}_{full\ scale}}{\mathrm{Re}_{model\ scale}}\right)^{m}. \qquad (7.1)$$

Using this equation as a basis, Billet et al. (1996) and the Cavitation Committee for the 21st ITTC presented an empirical equation for scaling rotor-blade-tip cavitation inception,

$$\sigma = constant\ \left(C_L\right)^{a}\left(\frac{\overline{W}_{tip}}{V_{ref}}\right)^{2} Re^{m}, \qquad (7.2)$$

where C_L is the average of the lift coefficients over some finite span of the rotor-blade tip, $\overline{W}_{tip}$ is the mean relative velocity at the rotor-blade tip, V_{ref} is a reference velocity (such as ship speed), and Re is the Reynolds number based on $\overline{W}_{tip}$ and the chord length of the rotor-blade tip. Billet et al. (1996) gave a theoretical value of two for the exponent a. Many researchers have suggested empirical values for the proportionality *constant* and the exponent m. Again, one must also take water-quality effects into account. Each organization has to determine their own empirical exponents and proportionality *constant* using their own comparisons between model- and full-scale results.

Billet et al. (2005) and the Specialist Committee on Cavitation Erosion on Propellers and Appendages on High Powered/High Speed Ships for the 24th ITTC presented an extensive overview of scaling effects for cavitation erosion. Most efforts to determine this type of scaling concentrate on pitting damage rate and the volume damage rate of controlled samples, with most researchers using the incubation period of material to analyze the flow and study the scaling effects.

Very little information is available for the Reynolds-number scaling effects for cavitation performance breakdown. Since cavitation breakdown is most often related to surface (sheet) cavitation, Reynolds-number scaling effects for cavitiaton breakdown are normally neglected.

Finally, numerical modeling of the behaviour of waterjet cavitation should theoretically allow for at least the Reynolds-number scaling effects, since one can use these models to simulate flows at both model-scale and full-scale Reynolds numbers. However, Appendix B will discuss the issues regarding numerical modeling of waterjet cavitation, and previous sections of this report have discussed these issues for cavitation in general. While practitioners will continue, and should continue, to employ numerical models to determine the behaviour of cavitation in waterjets, they need to be aware of the issues in using these models.

8 SUMMARY AND CONCLUSIONS

The 25th ITTC Specialist Committee on Cavitation reviewed the methods of predicting cavitation performance, a review that included a survey of the worldwide cavitation community. As confirmed by organizations that responded to the survey, experimental methods and model-scale testing still offer a primary method for predicting cavitation performance. Recent improvements have enhanced these experimental methods.

Particle image velocimetry (PIV) has become a mature technology for measuring non-cavitating flow fields, such as the inflows of propellers and rudders. With improved accuracy, PIV has become extremely useful in validating and supporting computational methods used for both non-cavitating and cavitating flows. Some very recent work has also involved using PIV with cavitation bubbles in the flow field. Improvements in nuclei measurements such as the use of interferometry have also been used in conjunction with PIV measurements.

For cavitating flows, improvements in high-speed video have aided the evaluation of unsteady pressure pulses, cavitation erosion, and cavity interactions. Also, the improved use of boroscopes during full-scale cavitation testing has enhanced the correlations with the model-scale testing used to predict cavitation performance.

Several computational methods have been used for a number of years to predict cavitation performance, methods that impact design and have been coupled with experimental models. These computational methods include empirical methods, potential-flow methods, and single-phase RANS solvers including techniques that couple different methods together. For instance, some groups in the cavitation community couple RANS solvers with potential-flow methods, and some couple RANS solvers with empirical methods.

While the methodology of potential-flow and single-phase RANS solvers have become quite mature, some groups have applied these methods to more and more complex applications. For instance, some groups have applied potential-flow methods to propeller flow fields interacting with a downstream rudder. Single-phase RANS solvers have become quite common, much easier to use, and show excellent results for simple flows. For more complex flows with many scales, analysts should proceed with caution using single-phase RANS solvers—since issues can arise regarding computational grids, turbulence models, and scale dissipation. For instance, the use of single-phase RANS solvers to accurately evaluate the static pressure within the core of a tip vortex can be very challenging, if not impossible.

Researchers have made significant strides in developing multiphase flow models for RANS solvers, and now most commercial RANS codes also have incorporated these models. However, RANS solvers with multiphase flow models have undergone very little validation, primarily because of a lack of quality experimental data. In fact, it is probably still premature to use these tools for the current prediction of full-scale cavitation performance on propellers and rudders. As more validation-quality experiments are performed in the future and compared with multiphase flow RANS simulations, these tools will become more mature.

Many flows, such as tip vortices, require better resolution of the turbulent structures. Researchers have made great progress in using large eddy simulation (LES) and detached eddy simulation (DES) to compute these flows. In the future, these computational methods will improve the prediction of vortex cavitation inception. Regarding unsteady cavitation, some researchers have just begun to use these advanced computational methods with multiphase flow models.

Clearly, several methods exist for predicting cavitation performance. However, cavitation performance includes different phenomena. For the inception of surface cavitation, most groups use single-phase RANS solvers or model-scale testing to obtain the correct inflow. With this correct inflow, many groups use potential-flow methods to predict surface cavitation inception. With the ability to simulate viscous-flow interactions, single-phase RANS solvers can offer improved predictions.

For the inception of vortex cavitation, many groups still use model-scale testing and an empirical scaling method to predict full-scale performance. Also, other groups use single-phase RANS solvers to compute parameters, such as propeller blade tip loading, and then use empirical methods to predict full-scale performance. Improvements in scaling methods and empirical methods will require more full-scale inception tests. Direct modeling of vortex cavitation inception will require better resolution of turbulent structures and flow unsteadiness, which may require methods such as LES or DES rather than RANS solvers.

The prediction of full-scale pressure fluctuations still relies almost exclusively on model-scale testing. While computational methods do quite well in simulating surface cavity areas, these methods are not yet ready to predict surface-cavitation-driven pressure fluctuations. Vortex-cavitation-driven pressure fluctuations are even more difficult to predict. Clearly, more validation-quality experiments are needed.

To predict cavitation erosion, all groups still utilize model-scale testing. Improvements in the use of high-speed video have helped to examine surface cavities and indicate the existence of fluctuations in void fraction. Experience is still necessary in correlating model-scale testing with full-scale erosion. Computationally, researchers have developed multiphase flow models to predict cavitation erosion. However, further research is required to achieve quantitative predictions.

Extensive cavitation leads to a major deterioration of thrust, torque, and total-head rise for propellers, waterjets, and pumps—referred to as cavitation breakdown. Most designers still use *rules* and empirical knowledge—and then make their final predictions using model-scale tests. Recent developments in using RANS solvers with multiphase flow models have made great advances, including comparisons with experimental data. In fact, some groups are now beginning to use these methods for the prediction of cavitation breakdown.

In addition to reviewing methods for predicting cavitation performance, the 25th ITTC Specialist Committee on Cavitation addressed cavitation behavior and the subsequent modeling of that behavior for the specific applications of rudders and waterjets. Billet et al. (2005) and the Specialist Committee on Cavitation Erosion on Propellers and Appendages on High Powered/High Speed Ships for the 24th ITTC previously addressed the key cavitation issue on rudders, namely cavitation erosion. Here, the 25th ITTC Specialist Committee on Cavitation extended this topic to cavitation on unconventional rudders and rudders downstream of highly-loaded propellers.

As discussed previously groups still utilize model-scale testing to predict cavitation erosion. On unconventional rudders and rudders downstream of highly-loaded propellers, one should test the complete unit of rudder *and* propeller, with a realistic propeller inflow, preferably generated by a complete ship model itself. Also, one should correctly model sharp edges and gaps. While one needs to test with a local Reynolds number of greater than 300,000, obtaining the correct local gap cavitation phenomena is still very challenging at model scale. Larger-scale part models may be necessary. In addition, one should investigate a wide range of rudder angles at model scale to satisfactorily evaluate cavitation erosion at full scale. Finally, high-speed video, improvements in the soft-ink method, and more full-scale cavitation observations will improve the prediction of cavitation erosion in the future.

While progress has been made, researchers have yet to develop a universally-accepted numerical method to predict cavitation erosion. Designers of rudders use empirical methods, potential-flow methods, and single-phase RANS solvers to obtain indirect information that guides their designs. However, model-scale testing is still necessary to predict rudder cavitation erosion.

Since the ITTC has never focused on waterjet cavitation issues, the 25th ITTC Specialist Committee on Cavitation provided a detailed summary of cavitation issues for the different components of a waterjet. The most critical cavitation issue for a waterjet involves cavitation breakdown of the pump, leading to a significant reduction in thrust. While cavitation breakdown can occur for high-speed operation, it may also occur at lower vehicle speeds and prevent the vehicle from getting over the "hump" created by high wave resistance and obtaining the desired high-speed operation. Cavitation erosion of the pump blades—which are normally manufactured using stainless steel to increase operational life—can also be an important issue. Cavitation vibration leading to blade fatigue—and cavitation noise can also be issues.

Cavitation can occur within a waterjet inlet as well. Waterjets that are well designed (or well matched) to operate with a given hull should only experience inlet cavitation when one operates the waterjet at an inlet velocity ratio (*IVR*) different from the design value. For these off-design values of *IVR*, flow separation and cavitation can occur on the inlet lip, or cutwater, and on the roof of the inlet.

Pump testing offers the most common method to predict pump cavitation breakdown, although the use of RANS solvers with multi-phase flow models are beginning to be used. Without the proper pump inflow, these pump tests are problematic to evaluate cavitation erosion and useless for evaluating cavitation vibration and noise. Waterjet system tests are used to observe inlet cavitation at various values of *IVR* and—depending on the test setup—to observe pump cavitation. Waterjet self-propulsion tests in a towing tank are not useful for cavitation testing.

Little specific information is available for waterjet cavitation issues, especially comparisons between full-scale data, model-scale data, and computational methods. In fact, most shipyards and model basins have not been asked to provide predictions of cavitation performance for waterjets. Instead, commercial waterjet manufacturers generally provide all design, analysis, and testing methods and results, especially with regard to cavitation performance—and for competitive reasons, these manufactures have been quite secretive.

9 RECOMMENDATIONS

The 25th ITTC Specialist Committee on Cavitation recommends that organizations adopt two new procedures and guidelines: (1) 7.5-02-03-03.7 on the "Prediction of Cavitation and Erosion Damage for Unconventional Rudders or Rudders behind Highly-Loaded Propellers" and (2) 7.5-02-03-03.8 on the "Modeling the Behavior of Cavitation in Waterjets."

10 REFERENCES

Abels, W., 2006, "Reliable Prediction of Propeller Induced Pulses on the Aftbody By Correlation Direct Calculation," Sixth International Symposium on Cavitation, CAV2006, Wageningen, The Netherlands.

Ait-Bouziad, Y., Farhat, M., Kueny, J.-L., Gueninoun, F., Avellan, F., and Miyagawa, K., 2003, "Physical Modeling and Simulation of Leading Edge Cavitation, Application to an Industrial Inducer," Fifth International Symposium on Cavitation (CAV2003), OS-6-014.

Arndt, R. E. A., Long, D. F., and Glauser, M. N., 1997, "Proper Orthogonal Decomposition of Pressure Fluctuations Surrounding a Turbulent Jet," Journal of Fluid Mechanics, Vol. 340, pp. 1-33.

Atsavapranee, P., Carneal, J., Etebari, A., and Percival, S., 2007, "Applications of Stereo Particle Image Velocimetry (SPIV) in Naval Hydrodynamics," 28th American Towing Tank Conference, Univ. of Michigan, Ann Arbor.

Bachert, B., Ludwig, G., Stoffel, B., and Baumgarten, S., 2005, "Comparison of Different Methods for the Evaluation of Cavitation Damaged Surfaces," Proceedings of the 2005 ASME Fluids Engineering Division Summer Meeting, FEDSM2005, pp. 553-560.

Bakir, F., Mejri-Chtioui, I., Kouidri, S., and Rey, R., 2003, "Hub Shape Effects under Cavitation on the Inducers Performance," Fifth International Symposium on Cavitation (CAV2003), OS-6-001.

Billet, M. L. (Chairman), 1996, "Report of the Cavitation Committee," 21st ITTC, Trondheim, Norway, pp. 63-126.

Billet, M. L. (Chairman), 2002, "Report of the Specialist Committee on Water Quality and Cvaitation," 23rd ITTC, Venice, Italy, pp. 459-491.

Billet, M. L. (Chairman), 2005, "Report of the Specialist Committee on Cavitation Erosion on Propellers and Appendages on High Powered/High Speed Ships," 24th ITTC, Edinburgh, United Kingdom, Vol. II, pp. 509-542.

Black, S., 2007, "Thrust Breakdown Characteristics of Conventional Propellers," Hydromechanics Departmental Report, NSWCCD-50-TR-2007/064.

Bulten, N. and Oprea, A. I, 2006, "Evaluation of McCormick's Rule for Propeller Tip Vortex Cavitation Inception Based on CFD Results," Sixth International Symposium on Cavitation (CAV2006), Wageningen, The Netherlands, Paper No. 28.

Burrill, L. C., 1943, "Developments in Propeller Design and Manufacture for Merchant Ships," Transactions, Institute of Marine Engineers, London, Vol. 55.

Burrill, L. C. and Emerson, A., 1963, "Propeller Cavitation: Further Tests on 16in. Propeller Models in the King's College Cavitation Tunnel," Transactions of the North East Coast Institution of Engineers and Ship Builders, Vol. 78, pp. 295-320.

Calcagno, G., Di Felice, F., Felli, M., and Pereira, F., 2005, "A Stereo PIV Investigation of a Propeller's Wake behind a Ship Model in a Large Free Surface Water Tunnel," Marine Technology Society Journal, Vol. 39, No. 2.

Carlton, J. S., and Fitzsimmons, P. A., 2006, "Full Scale Cavitation Observations Relating to Propeller Cavitation," Sixth International Symposium on Cavitation, CAV2006, Wageningen, The Netherlands.

Chahine, G. L., and Kalumuck, K., 2003, "Development of a Near Real Time Instrument for Nuclei Measurement: the ABS Acoustic Bubble Spectrometer," International Symposium on Cavitation Inception, Proceedings of FEDSM '03, Fourth ASME-JSME Joint Fluids Engineering Conference, Honolulu, HI.

Coutier-Delgosha, O., Fortes-Petella, R., Reboud, J. L., and Pouffary, B., 2002, "3D Numerical Simulation of Pump Cavitating Behavior," Proceedings of the 2002 ASME Fluids Engineering Division Summer Meeting, Montreal, Quebec, Canada.

Courtier-Delgosha, O. C., and Astolfi, J. A., 2003, "Numerical Prediction of the Cavitating Flow on a Two-Dimensional Symmetrical Hydrofoil With a Single Fluid Model," Fifth International Symposium on Cavitation (CAV2003), OS-1-013.

Coutier-Delgosha, O. C., Fortes-Patella, R. F., and Reboud, J. L., 2003a "Evaluation of the Turbulence Model Influence on the Numerical Simulation of Unsteady Cavitation," Transactions of the ASME, Journal of Fluid Engineering, Vol. 125, No. 1, pp.38–46.

Coutier-Delgosha, O., Perrin, J., Fortes-Patella, R., and Reboud, J. L., 2003b, "A Numerical Model to Predict Unsteady Cavitating Flow Behaviour in Inducer Blade Cascades," Fifth International Symposium on Cavitation (CAV2003), OS-4-005.

Coutier-Delgosha, O. C., Reboud, J. L., and Delannoy, Y., 2003c, "Numerical Simulation of the Unsteady Behaviour of Cavitating Flows," International Journal for Numerical Methods in Fluids, Vol. 42, pp.527–548.

Damaschke, N., Nobach, H., and Tropea, C., 2006, "Global Phase Doppler Technique for Size and Velocity Measurements," DLR-Mitteilung, No. 3, pp. 1055-1067.

Dang, J., 2004, "Improving Cavitation Performance with New Blade Sections for Marine Propellers," International Shipbuilding Progress, Vol. 51, No. 4, pp. 353-376.

Di Felice, F., Di Florio, D., Felli, M., and Romano, G. P, 2004, "Experimental Investigation of the Propeller Wake at Different Loading Conditions by Particle Image Velocimetry," Journal of Ship Research, Vol. 48, No. 2.

Dreyer, J. J., Koncoski, J. J., Zierke, W. C., and Willits, S. M., 2006, "Experimental Verification of Blade-Shape Optimization for Improved Off-Design Cavitation Performance," Proceedings of the Eleventh International Symposium of Transport Phenomena and Dynamics of Rotating Machinery (ISROMAC-11), Honolulu, Hawaii, USA.

Dular, M., Bachert, R., Stoffel, B., and Sirok, B., 2003, "Numerical and Experimental Study of Cavitating Flow on 2D and 3D Hydrofoils," Fifth International Symposium on Cavitation (CAV2003), GS-9-011.

Dular., M., Bachert, R., and Stoffel, B., 2006a, "Experimental and Numerical Investigation of Swept Leading Edge Influence on the Developed Cavitation," Sixth International Symposium on Cavitation (CAV2006), Wageningen, The Netherlands, Paper No. 102.

Dular, M., Širok, B. and Stoffel, B., 2006b, "Experimental and Numerical Modelling of Cavitation Erosion," Sixth International Symposium on Cavitation (CAV2006), Wageningen, The Netherlands, Paper No. 55.

Dupont, P. and Casartelli, E., 2002, "Numerical Prediction of the Cavitation in Pumps," Proceedings of the 2002 ASME Fluids Engineering Division Summer Meeting, Montreal, Quebec, Canada.

Edge. B., 2007, "An Analytical and Numerical Study of Cavitation Scale Effects in High-Reynolds Number Circular Jet Flows," Ph.D. Dissertation, Department of Mechanical Engineering, The Pennsylvania State University.

Escaler, X., Farhat, M., Egusquiza, E., and Avellan, F., 2007, "Dynamics and Intensity of Erosive Partial Cavitation," ASME Journal of Fluids Engineering, Vol. 129, pp. 886-893.

Falcao de Campos, J., Vaz, G., and Bosschers, J., 2006, "Influence of the Reduced Frequency on the 2-D Partial Sheet Cavitation Behavior for a Foil in a Gust," Sixth International Symposium on Cavitation (CAV2006), Wageningen, The Netherlands, Paper No. 113.

Felli, M., Di Felice, F., Guj, G., and Camussi, R., 2006, "Analysis of the Propeller Wake Evolution by Pressure and Velocity Phase Measurements," Experiment in Fluids, Vol. 41, pp. 441-451.

Fine, N. E. and Kinnas, S. A., 1993, "A Boundary-Element Method for the Analysis of the Flow around 3-D Cavitating Hydrofoils, Journal of Ship Research, Vol. 37, pp. 213-224.

Flores, N. G., 2006, "Head Drop of Spatial Turbopump Inducer," Sixth International Symposium on Cavitation (CAV2006), Wageningen, The Netherlands, Paper No. 108.

Foeth, E.-J., and Terwisga, T. van, 2006, "The Structure of Unsteady Cavitation: Part II Applying Time-Resolved PIV to Attached Cavitation," Sixth International Symposium on Cavitation, CAV2006, Wageningen, The Netherlands.

Friesch, J., 2006, "Rudder Erosion Damages Caused by Cavitation," 6th International Symposium on Cavitation (CAV2006), Wageningen, The Netherlands, Invited Paper.

Frobenius, M., Schilling, R., Friedrichs, J., and Kosyna, G., 2002, "Numerical and Experimental Investigations of the Cavitating Flow in a Centrifugal Pump Impeller," Proceedings of the 2002 ASME Fluids Engineering Division Summer Meeting, Montreal, Quebec, Canada.

Frobenius, M., Schilling, R., Bachert, R., Stoffel, B., and Ludwig, G., 2003, "Three-Dimensional Unsteady Cavitation Effects on a Single Hydrofoil and in a Radial Pump - Measurements and Numerical Simulations: Part Two: Numerical Simulation," Fifth International Symposium on Cavitation (CAV2003), GS-9-004.

Fry, D. J., 2007, "Scanning LDV for Tow Tank Wake Surveys," 28th American Towing Tank Conference, University of Michigan, Ann Arbor.

Fukaya, M., Okamura, T., Tamura, Y., and Matsumoto, Y., 2003, "Prediction of Cavitation Performance of Axial Flow Pump by Using Numerical Cavitating Flow Simulation with Bubble Flow Model," Fifth International Symposium on Cavitation (CAV2003), OS-6-012.

Fukaya, M., Tamura, Y., and Matsumoto, Y., 2006, "Prediction of Cavitation Intensity and Erosion in Centrifugal Pump Based on Detailed Bubble Behavior Simulated Using Bubble Flow Model," The 11th International Symposium on Transport Phenomena and Dynamics of Rotating Machinery (ISROMAC-11), Honolulu, Hawaii.

Han K-J., Bark, G., Larsson, L., and Regnstrom, B., 2006, "A Procedure for Optimizing Cavitating Propeller Blades in a Given Wake," Ship Technology Research, Vol. 53, No. 1, pp. 39-52.

Hosangadi, A., Ahuja, V., and Ungewitter R. J., 2006, "Numerical Study of a Flat Plate Inducer: Comparison of Performance in Liquid Hydrogen and Water," Sixth International Symposium on Cavitation (CAV2006), Wageningen, The Netherlands, Paper No. 82.

Hoyt III, J. G. (Chairman), 1999, "Report of the Specialist Committee on Waterjets," 22nd ITTC, Seoul, South Korea and Shanghai, China, pp. 587-613.

Hsiao, C.-T. and Chahine, G., 2004, "Prediction of Tip Vortex Cavitation Inception Using Coupled Spherical and Nonspherical Bubble Models and Navier–Stokes Computations," Journal of Marine Science and Technology, Vol. 8, No. 3, pp. 99-108.

Huuva, T., 2008, "Large Eddy Simulation of Cavitating and Non-Cavitating Flow," Ph.D. Thesis, Department of Shipping and Marine Technology, Chalmers University of Technology, Göteborg, Sweden.

Iga, Y., Nohmi, M., and Goto, A., 2003, "Numerical Study of Sheet Cavitation Breakoff Phenomenon on a Cascade Hydrofoil," Transactions of the ASME, Journal of Fluids Engineering, Vol. 125, No. 4, pp. 643-652.

Iga, Y., Nohml, M., and Goto, A., 2004, "Numerical Analysis of Cavitation Instabilities Arising in the Three-Blade Cascade," Transactions of the ASME, Journal of Fluids Engineering, Vol. 126, No. 3, pp. 419-430.

Jessup, S. D (Chairman), 2002, "Report of the Propulsion Committee," 23rd ITTC, Venice, Italy, Vol. I, pp. 99-151.

Kawamura, T. and Sakoda, M., 2003, "Comparison of Bubble and Sheet Cavitation Models for Simulation of Cavitating Flow over a Hydrofoil," Fifth International Symposium on Cavitation (CAV2003), OS-1-008.

Kawamura, T., Takekosi, Y., Yamaguchi, Y., Minowa, T., Maeda, M., Fujii, A., Kimura, K., and Taketani, T., 2006, "Simulation of Unsteady Cavitating Flow around Marine Propeller Using a RANS CFD Code," Sixth International Symposium on Cavitation (CAV2006), Wageningen, The Netherlands, Paper No. 173.

Kawamura, T. and Kiyokawa, T., 2008, "Numerical Prediciton of Hull Surface Pressure Fluctuation Due to Propeller Cavitation," Conference Proceedings of the Japan Society of Naval Architects and Ocean Engineers, Nagasaki, Japan, No. 6.

Kehr, Y-Z., and Kao, J-H., 2005, "Numerical Prediction of the Blade Rate Noise Induced by Marine Propellers," Journal of Ship Research, Vol. 48, No. 1, pp. 1-14.

Kim, J., Paterson, E. G., and Stern, F., 2006, "RANS Simulation of Ducted Marine Propulsor Flow Including Subvisual Cavitation and Acoustic Modeling," Transactions of the ASME, Journal of Fluids Engineering, Vol. 128, No. 4, pp. 799-811.

Kimura, T., Yoshida, Y., Hashimoto, T., and, Shimagaki, M., 2006, "Numerical Simulation for Unsteady Cavitating Flow in a Turbopump Inducer," Sixth International Symposium on Cavitation (CAV2006), Wageningen, The Netherlands, Paper No. 41.

Kinnas, S. A., Lee, H., Sun, H., and He, L., 2007, "Performance Prediction of Single or Multi-Component Propulsors Using Coupled Viscous/Inviscid Methods," 10th International Symposium on Practical Design of Ships and Other Floating Structures (PRADS), American Bureau of Shipping, Houston, TX, U.S.A.

Koronowicz, T., and Szantyr, J. A., 2006, "Vortex Cavitation as a Source of High Level Acoustic Pressure Generated by Ship Propellers," Acta Acustica united with Acustica, Vo. 92, pp. 175-177.

Kunz, R. F, Lindau, J. W., Peltier, L. J., and Kaday, T. A., 2003, "Detached Eddy Simulation of Developed Cavitating Flows," Fifth International Symposium on Cavitation (CAV2003), OS-1-012.

Lee, S-K., and Chen, H-C., 2005, "The Influence of Propeller/Hull Interaction on Propeller Induced Cavitating Pressure," Proceedings of the 15th International Offshore and Polar Engineering Conference, Seoul, Korea, pp. 596-603.

Lee, H., and Kinnas, S. A., 2004, "Application of a Boundary Element Method in the Prediction of Unsteady Blade Sheet And Developed Tip Vortex Cavitation on Marine Propellers," Journal of Ship Research, Vol. 48, No. 1, pp. 15-30.

Leroux, J.-B., Coutier-Delgosha, O., Astolfi, J. A., 2003, "A Joint Experimental and Numerical Study of Mechanisms Associated to Instability of Partial Cavitation on Two-Dimensional Hydrofoil," Fifth International Symposium on Cavitation (CAV2003), GS-9-006.

Leroux, J. B., Coutier-Delgosha, O., and Astolfi, J. A., 2005, "A Joint Experimental and Numerical Study of Mechanisms Associated to Instability of Partial Cavitation on Two-Dimensional Hydrofoil," Physics of Fluids, Vol. 17, No. 5, p. 52101.

Li, D.-Q., 2006, "Validation of RANS Predicitons of Open Water Performance of a Highly Skewed Propeller with Experiments," Conference of Global Chinese Scholars on Hydrodynamics (CCSH).

Ligtelijn, J. T., Wijngaarden, H. C. J. van, Moulijn, J. C., and Verkuyl, J. B., 2004, "Correlation of Cavitation: Comparison of Full-Scale Data with Results of Model Tests and Computations," Transactions of the Society Of Naval Architects and Marine Engineers, Vo. 112, pp. 80-110.

Lindau, J. W., Boger, D. A., Medvitz, R. B., and Kunz, R. F., 2005, "Propeller Cavitation Breakdown Analysis," Journal of Fluids Engineering, Vol. 127, pp. 995-1002.

Longo, J., Gui, L., and Stern, F., 2004, "Ship Velocity Fields," Chapter 3: PIV and Water Waves, Advances in Costal and Ocean Engineering, Vol. 9, World Scientific, pp. 119-180.

McCormick, B. W., 1962, "On Cavitation Produced by a Vortex Trailing from a Lifting Surface," Journal of Basic Engineering, Transactions of the American Society of Mechanical Engineers (ASME), pp. 369-379.

Miller, W. and Wilczynski, L., 2006, "Model - Full Scale Correlations of the Cavitation Erosion of Ship Propeller and Rudder - a Container Vessel Study," Sixth International Symposium on Cavitation

(CAV2006), Wageningen, The Netherlands, Paper No. 124.

Nohmi, M., Goto, A., Iga, Y., and Ikohagi, T., 2003, "Cavitation CFD in a Centrifugal Pump," Fifth International Symposium on Cavitation (CAV2003), OS-4-010.

Oberkampf, W. L., Trucano, T. G., and Hirsch, C., 2004, "Verification, Validation, and Predictive Capability in Computational Engineering and Physics," Applied Mechanics Review, Vol. 57, No. 5, pp. 345-384.

Okita, K., Matsumoto, Y., and Kamijo, K., 2003, "Numerical Analysis for Unsteady Cavitating Flow in a Pump Inducer," Fifth International Symposium on Cavitation (CAV2003), OS-4-012.

Oweis, G. F., and Ceccio, S. L., 2005, "Instantaneous and Time-Averaged Flow Fields of Multiple Vortices in the Tip Region of a Ducted Propulsor," Experiments in Fluids, Vol. 38, pp. 615-635.

Palero, V., Lobera, J., and Arroyo, M. P., 2005, "Digital Image Plane Holography (DIPH) for Two-Phase Flow Diagnostics in Multiple Planes," Experiments in Fluids, Vol. 39, No. 2, pp. 397-406.

Patella, R. F., Reboud, J. L., and Archer, A., 2000, "Cavitation Damage Measurement by 3D Laser Profilometry," Wear, Vol. 246, Nov. pp. 59-67.

Patella, R. F. and Reboud, J.-L., 2006, "Experiments and Modelling of Cavitating Flows in Venturi Part II: Unsteady Cavitation," Sixth International Symposium on Cavitation (CAV2006), Wageningen, The Netherlands, Paper No. 109.

Pereira, F., Salvatore, F., Di Felice, F., 2004, "Measurement and Modeling of Propeller Cavitation in Uniform Inflow," Journal of Fluids Engineering, Transactions of the ASME, Vol. 126, No. 4, pp. 671-679.

Persson, T., Bark, G., Bensow, R., Berchiche, N., and Fureby, C., 2006, "Large Eddy Simulation of the Cavitating Flow around a Wing Section," Sixth International Symposium on Cavitation (CAV2006), Wageningen, The Netherlands, Paper No. 45.

Philipp, A., and Lauterborn, W., 1988, "Damage of Solid Surfaces by Single Laser-Produced Cavitation Bubbles," Acta Acustica, Vol. 83, No. 2, pp. 223-227.

Pouffary, B., Fortes-Patella, R., and J.-L. Reboud, J.-L., 2003, "Numerical Simulation of Cavitating Flow around a 2D Hydrofoil: A Barotropic Approach", Fifth International Symposium on Cavitation (CAV2003), OS-1-005.

Qin, Q., Song, C. C. S., and Arndt, R. E. A, 2003, "A Virtual Single-Phase Natural Cavitation Model and Its Application to CAV2003 Hydrofoil," Fifth International Symposium on Cavitation (CAV2003), OS-1-004.

Rhee, S. H., Kawamura, T., and Li, H., 2005, "Propeller Cavitation Study Using an Unstructured Grid Based Navier-Stoker Solver," Transactions of the ASME, Journal of Fluids Engineering, Vol. 127, pp. 986-994.

Rhee, S. H., Oh, J.-K., Lee, S.-H., and Kim, H., 2007, "Development of Rudder Cavitation Suppression Devices and its Concept Verification through Experimental and Numerical Studies," 10th International Symposium on Practical Design of Ships and other Floating Structures (PRADS), Houston, Texas.

Rolland, J., Boitel, G., Barre, S., Goncalves, E., and Patella, R. F., 2006, "Experiments and Modelling of Cavitating Flows in Venturi Part I: Stable Cavitation," Sixth International Symposium on Cavitation (CAV2006), Wageningen, The Netherlands, Paper No. 110.

Saito, Y., Nakamori, I., Ikohagi, T., 2003, "Numerical Analysis of Unsteady Vaporous Cavitating Flow around a Hydrofoil," Fifth International Symposium on Cavitation (CAV2003), OS-1-006.

Seol, H., Suh, J–C., and Lee, S., 2005, "Development of Hybrid Method for the Prediction of Underwater Propeller Noise," Journal of Sound and Vibration, Vol. 288, No. 1-2, pp. 345-360.

Shaw, S. J., Schiffers, W. P., Gentry, T. P., and Emmony, D. C., 2000, "The Interaction of a Laser-Generated Cavity with a Solid Boundary," Journal of the Acoustical Society of America, Vol. 107, No. 6, pp. 3065-3072.

Shen, Y. T., Jessup, S. D., and Gowing, S. 2001, "Tip Vortex Cavitation Inception Logarithmic Scaling," NSWCCD-50-TR-2001/060, Oct. 2001.

Singhal, A.K., Athavale, M.M., Li, H.Y., Jiang, Y., 2002, "Mathematical Basis and Validation of the Full Cavitation Model," Journal of Fluids Engineering, Vol. 124, pp. 617-624.

Soyama, H., Lichtarowicz, A., Momma, T., and Williams, E. J., 1998, "A New Calibration Method for Dynamically Loaded Transducers and Its Application to Cavitation Impact measurement," Transactions of the ASME, Vol. 120, pp. 712-718.

Spalart, P. R. and Allmaras, S. R., 1994, "One-Equation Turbulence Model for Aerodynamic Flows," La Recherche Aerospatiale, No. 1, pp. 5-21.

Streckwall, H., and Salvatore, F., 2007, "Results from the Wageningen 2007 Workshop on Propeller Openwater Calculations Including Cavitation," *Virtue*, Workshop On Propeller RANS Calculations, Conditions and Requested Results for Non-Cavitating and Cavitating RANS Analysis of INSEAN Propeller E779A (Version 4), Wageningen, Netherlands.

Takekoshi, Y., Kawamura, T., Yamaguchi, H., Maeda, M., Ishi, N., Kimura, K., Taketani, T., and Fuji, A., 2005, "Study on the Design of Propeller Blade Sections using the Optimization Algorithm," Journal of Marine Science and Technology, Vol. 10, No. 2, pp. 70-81.

Takekoshi, Y. and Kawamura, T., 2006, "Comparison of Cavitation Models for Simulation of Cavitating Flow over a Hydrofoil," Sixth International Symposium on Cavitation (CAV2006), Wageningen, The Netherlands, Paper No. 174.

van derHout, I., Tukker, J., and Gent, A., van, 2006, "New Developments on Full Scale Cavitation Observations," Sixth International Symposium on Cavitation, CAV2006, Wageningen, The Netherlands.

van Rijsbergen, M. X. and van Terwisga, T. J. C., 2000, "On the Maximum Thrust Density of Propellers," NCT'50 International Conference on Propeller Cavitation, Newcastle, United Kingdom, pp. 97-119.

van Wijngaarden, H. C. J. van, Brouwer, J., and Zijlstra, M.., 2006, "A Spatial Extrapolation Technique for Sparse Measurements of Propeller-Induced Hull Pressures Using an Inverse Acoustic Boundary Element Method," Sixth International Symposium on Cavitation (CAV2006), Wageningen, The Netherlands, Paper No. 93.

Wang, Y. C., Huang, C. H., Lee, Y. C., and Tsai, H. H., 2006, "Development of a PVDF Sensor Array for Measurement of the Pressure Generated by Cavitation Bubble Collapse," Experiments in Fluids, Vol. 41, pp. 365-373.

Wang, G. and Ostoja-Starzewski, M., 2007, "Large Eddy Simulation of a Sheet/Cloud Cavitation on a NACA0015 Hydrofoil," Applied Mathematical Modelling, Vol. 31, No. 3, pp. 417-448.

Watanabe, T., Kawamura, T., Takekoshi, Y., Maeda, M., and Rhee, S.-H., 2003, "Simulation of Steady and Unsteady Cavitation on a Marine Propeller using a RANS CFD code," Fifth International Symposium on Cavitation (CAV2003), GS-12-004.

Wienken, W., Stiller, and J., Keller, 2006, "A Method to Predict Cavitation Inception Using Large-Eddy Simulation and its Application to the Flow Past a Square Cylinder," Transactions of the ASME, Journal of Fluids Engineering, Vol. 128, No. 2, pp. 316-326.

Wosnik, M. and Arndt, R. E. A., 2006, "Identification of Large Scale Structures in the Wake of Cavitating Hydrofoils Using LES and Time Resolved PIV," Sixth International Symposium on Cavitation (CAV2006), Wageningen, The Netherlands, Paper No. 67.

Wu, J., Utturkar, Y. and Shyy, W., 2003 "Assessment of Modeling Strategies for Cavitating Flow around a Hydrofoil," Fifth International Symposium on Cavitation (CAV2003), OS-1-007.

Yamada, H., Yoshida, Y., Shimagaki, M., Watanabe, M., Hasegawa, S., Hashimoto, T., Kimura, T., and Uchiumi, M., 2003, "Performance of a Tandem Inducer under Non-cavitating and Cavitating Conditions," Fifth International Symposium on Cavitation (CAV2003), OS-4-008.

Xiong, Y. L., Gao, Y., and An, W. G., 2006, "Comparisons of Turbulence Models in Predicting Unsteady Supercavitating Flow," Sixth International Symposium on Cavitation (CAV2006), Wageningen, The Netherlands, Paper No. 25.

APPENDIX A: UNCONVENTIONAL RUDDERS AND RUDDERS BEHIND HIGHLY-LOADED PROPELLERS

Appendix A addresses the questions "What is an unconventional rudder?" and "What is a highly-loaded propeller?"

A.1 Unconventional Rudders

An estimated 95% (or more) of the sea-going ships sail with symmetric spade or semi-spade rudder(s) behind their propeller(s). Regarding these types of rudders as the conventional solution, the committee will consider everything else as an unconventional rudder arrangement.

In order to classify the large variety of unconventional rudders, it might be most reasonable to do this by distinction of the intended effect responsible for the unconventionality. In doing so, the committee will describe distinct classes of unconventional rudders.

Active Generation of Additional Rudder Forces. One class of rudders is equipped with a special device that actively generates an additional side-force vector. Figure A.1 shows an example of this so-called *active rudder*, where a motor-propeller unit integrated within the movable rudder blade generates this additional side force.

Conversely, Figure A.2 shows a r*udder rotor*, which generates this force from a rotating cylinder integrated into the rudder leading edge, causing the well-known Magnus effect. Additionally, this rotating cylinder accelerates the flow and prevents early flow separation on the rudder suction side.

Figure A.1 Active rudder.

Figure A.2 Rudder rotor.

Passive Generation of Higher Rudder Forces. Another class of rudders is designed to produce larger rudder forces without additional energy input. Figure A.3 shows such a rudder, which achieves a larger force by the reduction of losses. Here, end plates prevent an unintended pressure difference equalization around the upper and lower surface ends of a semi-spade rudder blade. Other losses may be involved in the pressure equalizing flow through the rudder gaps. Rhee et al. (2007) described a solution featuring gap flow suppressing wedges installed at the vertical gaps of a semi-spade rudder to overcome this problem. They report a lift force increase of more than 40 %.

Figure A.3 Rudder with end plates.

Figure A.4 shows another unconventional rudder that increases the side force with an additional flap at the rudder trailing edge—a flap that generates a more favorable static-pressure distribution in the chordwise direction.

Figure A.4 Full-spade flap rudder.

Whether actively or passively generating increased side forces, these unconventional rudders achieve the higher forces at the expense of higher resistance.

Improvement of Propulsion Performance. As a completely different approach, one can design an unconventional rudder geometry to increase the propulsion performance of a vessel. Figure A.5 shows a typical example for this class of rudders: the asymmetric rudder blade, which recovers energy from the swirl downstream of the propeller. These rudders can either be of semi-spade or full-spade type. The same working principle stands behind the rudder fin, which features wings attached to the rudder.

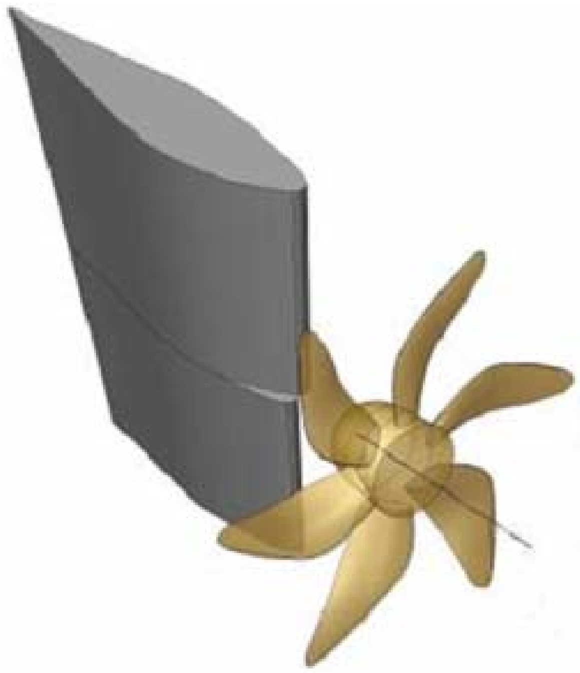

Figure A.5 Twisted full-spade rudder.

The *Costa Bulb*, shown in Figure A.6, represents another possible application. This rudder aims to reduce losses involved in the propeller hub vortex. This bulb is normally installed on a movable spade rudder blade, which means that there must be a disadvantageous gap between the propeller hub and the bulb. Also, the so-called *High-Efficiency Rudder*, shown in Figure A.7, is a consequence of further development of this working principle, applied on a horn-type rudder.

Improvement of Cavitation Performance. Finally, one can consider another class of unconventional rudders with the intention of avoiding cavitation problems on the rudder itself. The previously described twisted rudder, as shown in Figure A.5, gives an example in which one considers this cavitation requirement during the design phase of the rudder. Besides its energy recovering effect, this rudder also reduces rudder leading-edge cavitation, because the rudder profile is better adjusted to the propeller swirl. Figure A.8 shows a very complicated geometry developed after the design and original fabrication of a conventional symmetrical semi-spade rudder that suffered from severe rudder cavitation erosion. Geometry modifications such as this one—or just simple scissor plates or spoilers—may convert a conventional rudder into an unconventional one.

Figure A.6 Full-spade rudder with a *Costa Bulb*.

Figure A.7 High-efficiency rudder.

Park et al. (2007) described numerical investigations of slot bars, scissor plates, and special rudder horn geometries to achieve better cavitation performance with a conventional semi-spade rudder. The gap flow suppressing wedges proposed by Rhee et al. (2007) for lift force improvement (as described previously) may also be understood as a contribution to gap cavitation prevention. Additionally, the end plate shown in Figure A.3 also helps to improve the cavitation behavior by delaying or moving the tip vortex at the rudder sole.

Figure A.8 Semi-spade rudder modified to reduce cavitation.

A.2 Highly-Loaded Propellers

Propeller loading is normally measured by the thrust-loading coefficient, C_{Th}, expressing the propeller-generated energy increase of the fluid passing through the propeller disc, related to the initial kinetic energy of this fluid. C_{Th} is important for the rudder cavitation behavior, since the acceleration of the flow by the propeller directly depends on the thrust-loading coefficient. From momentum theory, the axial flow speed behind the propeller, V_{behind}, is

$$V_{behind} = \left(1 + C_{Th}\right)^{1/2} \cdot V_A, \tag{A.1}$$

where V_A is the speed of advance (as determined from open-water propeller tests). In other words, with a thrust-loading coefficient of C_{Th} = 3, for example, the incoming flow speed would be doubled by the propeller action. According to propeller theory, the induced velocities are not axially directed, but they are more or less perpendicular to the propeller blades (strictly speaking, they are perpendicular to the helical sheet of free vortices). This means that the flow behind the propeller is not only axially accelerated, but it gets an additional swirl in the same direction as the propeller rotation. Thus, a higher thrust loading gives a stronger amount of swirl downstream of the propeller—or a stronger amount of cross flow within the rudder inflow.

Unfortunately, the thrust-loading coefficient is normally not known in the early design stage of a ship, since the thrust requirement and wake fraction (and, for this reason, V_A) are unknown. A practical classification of propeller loads should be based on the power density value—the power flux through the propeller disc—as shown in Figure A.9. The values plotted in this figure are known in an early design stage and correlate quite well with the much more precise thrust-loading coefficient. The values displayed in Figure A.9 were taken from the Hamburg Ship Model Basin's cavitation testing statistics.

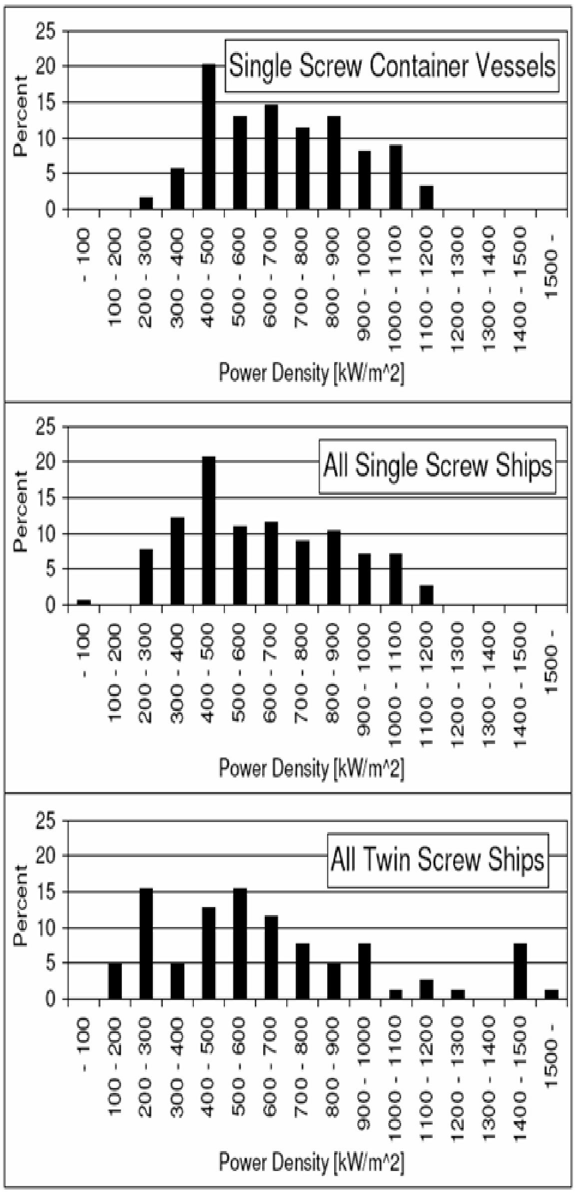

Figure A.9 Propeller loads (testing statistics from the Hamburg Ship Model Basin).

Figure A.9 shows that two thirds of all seagoing ships—with either one or two propellers—have a power density of not more than 800 kW/m^2. For single-screw ships, the usual values range from 400 kW/m^2 to 500 kW/m^2—while for twin-screw vessels, the typical power densities are more widespread. Nevertheless, a pragmatic definition for a highly-loaded propeller would be one with more than 800 kW delivered power per square meter of disc area.

A.3 References.

Park, S., Heo, J., and Yu, B., 2007, "Numerical Study on Horn Rudder Section to Reduce Gap Cavitation," 10th International Symposium on Practical Design of Ships and other Floating Structures (PRADS), Houston, Texas.

Rhee, S. H., Oh, J.-K., Lee, S.-H., and Kim, H., 2007, "Development of Rudder Cavitation Suppression Devices and its Concept Verification through Experimental and Numerical Studies," 10th International Symposium on Practical Design of Ships and other Floating Structures (PRADS), Houston, Texas.

APPENDIX B: WATERJET CAVITATION ISSUES

To date, the ITTC's work on waterjets has focused on providing procedures for the determination of the powering characteristics of waterjet-propelled vessels. Kruppa et al. (1996) and the Specialist Committee on Waterjets for the 21st ITTC proposed a *momentum flux* method. They also discussed the *direct thrust measurement* method, which they felt required further evaluation. Later, Hoyt et al. (1999) and the Specialist Committee on Waterjets for the 22nd ITTC recommended three types of tests for determining the powering characteristics: self-propulsion tests, waterjet system tests, and pump tests. Within a towing tank, the self-propulsion tests would provide the required flow rate, waterjet thrust, and effective waterjet system power—including waterjet/hull interaction factors. The waterjet system tests would then determine the system characteristics in terms of the flow rate, head, torque, and required power. Finally, the pump tests would determine the hydraulic characteristics of the pump without the flow distortion caused by the intake and hull boundary layer.

Van Terwisga et al. (2002) and the Specialist Committee on Waterjet Test Procedures for the 23rd ITTC set out to have several ITTC members conduct a series of these three standardization tests, with a special emphasis on including accompanying results from CFD. This work became possible through the teaming with a project sponsored by the United States Office of Naval Research (ONR) and administered by the Gulf Coast Region of Maritime Technology Center, situated at the University of New Orleans. With a delay in the delivery of the models sponsored by the Gulf Coast Project, van Terwisga et al. (2005) and the Specialist Committee on Waterjet Test Procedures for the 24th ITTC finished the work from the previous committee, thus completing the ITTC effort to provide procedures for the determination of the powering characteristics of waterjet-propelled vessels. In addition, Wilson et al. (2003) provided the final review of the Gulf Coast Project.

As pointed out by van Terwisga et al. (2005), the 24th ITTC Specialist Committee on Waterjet Test Procedures—and the previous committees—deliberately disregarded the effect of cavitation on the powering characteristics and possible erosion effects from the scope of their work. They assumed for their work that cavitation in the pump or intake during operation of the vessel does not affect the powering characteristics. However, they did suggest that this assumption should be checked with the waterjet manufacturer for each individual application.

Appendix B provides a fairly detailed description of cavitation issues related to waterjets.

B.1 Waterjet Cavitation Issues

Waterjets must produce a thrust that overcomes the various components of resistance, or drag, of the vessel. All vessels experience some resistance as the superstructure—the portion of the vessel above the water surface—moves through the air, but this resistance is usually small relative to the other components. The portion of the vessel that stays under the water surface experiences a viscous resistance. At low speeds—or low Froude numbers—this viscous resistance dominates the total resistance of the vessel, and it increases approximately with the square of the vehicle speed. As the speed—or the Froude number—increase, wave resistance becomes a higher percentage of the total resistance with the formation of waves that follow the ship, known as the Kelvin wake. At some critical speed or "hump" speed the wave resistance exceeds the viscous resistance. In this region, most high-speed hulls differ from displacement hulls. For high-speed hulls, hydrodynamic lift becomes important, and the hull begins to plane, and the wave drag decreases—producing a "hollow" in the resistance curve, as shown in Figure B.1. Also, Figure B.1 shows how a rough sea increases wave drag—and, thus, the total resistance of the vessel.

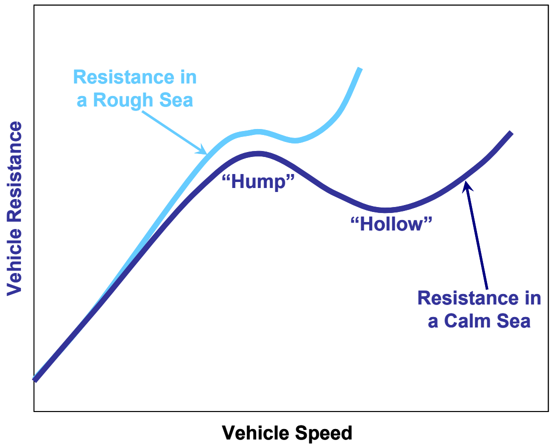

Figure B.1 Generic resistance curves for a high-speed vehicle.

For these high-speed planing or surface-effect ships, Garrett (1967) and Wislicenus (1973) both report that the thrust requirements of a waterjet system in traversing the "hump" region can be nearly as high—and possibly even higher—than at the cruising speed. As will be discussed later in this report, waterjet pumps require a minimum absolute pressure at the pump inlet—or a net positive suction head—to avoid cavitation. This net positive suction head, *NPSH*, increases with vehicle speed—so it is very much lower at the "hump" speed than at the cruising speed, increasing the tendency for the pump to cavitate. Therefore, for some vessels operating with a waterjet propulsion system, the thrust requirements within the "hump" region can dictate the design or selection of the waterjet—and, in many cases, the waterjet pump will operate in a cavitating condition during transit through this "hump" region.

One designs or selects a shaft speed, Ω, for the waterjet pump that coincides with the normal rating of the engine. The resulting net thrust curve for the waterjet propulsion system intersects the resistance curve (for a specified sea state), giving the speed of the vessel, as shown in Figure B.2. This figure also shows that one may be able to increase the shaft speed even further—for a short amount of time—but an engine power limit does exist.

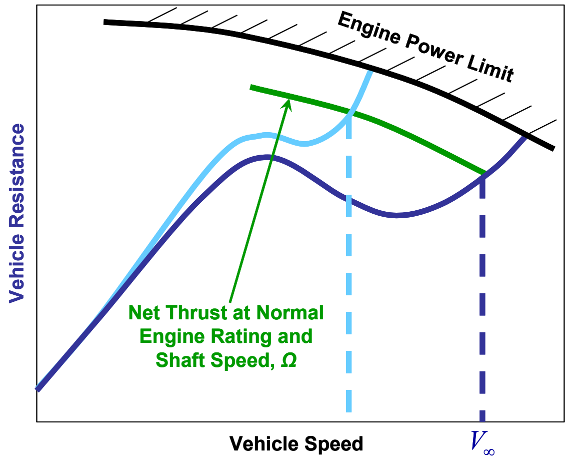

Figure B.2 Generic resistance curves for a high-speed vessel, with a generic net thrust curve for a waterjet.

Pump cavitation can be characterized by a parameter called the suction specific speed, N_{SS} (which will be defined later). Figure B.3 shows a line of constant N_{SS} added to the resistance and thrust curves. Operating at a higher value of N_{SS} will result in cavitation breakdown and a significant decrease in total-head rise and net thrust, meaning that the pump will no longer absorb the horsepower. Figure B.3 shows this pump suction limit. If this limiting curve of constant N_{SS} moved down and to the right on Figure B.3, one may get to the point where cavitation breakdown on the pump would prevent the vehicle from getting over the "hump" and reaching the desired cruise speed.

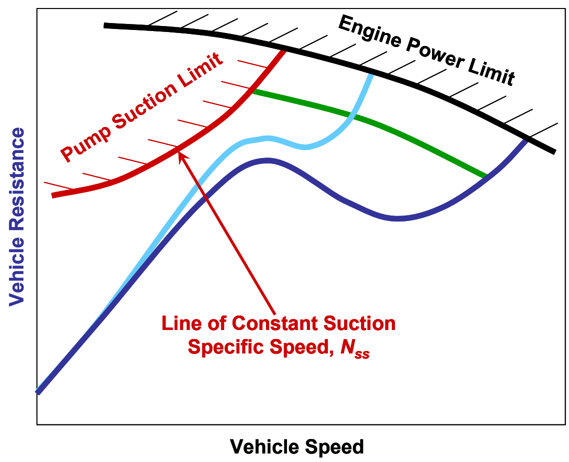

Figure B.3 Generic resistance and thrust curves for a high-speed vessel powered by a waterjet, with a limiting value of suction specific speed for cavitation breakdown.

As pointed out by Allison (1993), some waterjet manufacturers indicate zones of operation on their waterjet pump maps. Figure B.4 shows these zones. This figure adds additional net thrust curves (for different shaft speeds) and curves of constant N_{ss} to Figure B.3. Operation within Zone 1 is unrestricted, probably with only some intermittent cavitation. The pressure fluctuations associated with this intermittent cavitation could increase vibration and noise, which is probably not an issue with most applications. For operation in rough weather or at overload displacement, one could operate in Zone 2, which probably includes developed cavitation. This developed cavitation would further increase vibration and noise, and it could lead to some erosion. Operation in Zone 3 (or beyond the pump suction limit) is prohibited and would include significant vapor cavities. Operation here would not only increase cavitation erosion, vibration, and noise, but it would also lead to complete cavitation breakdown of the thrust.

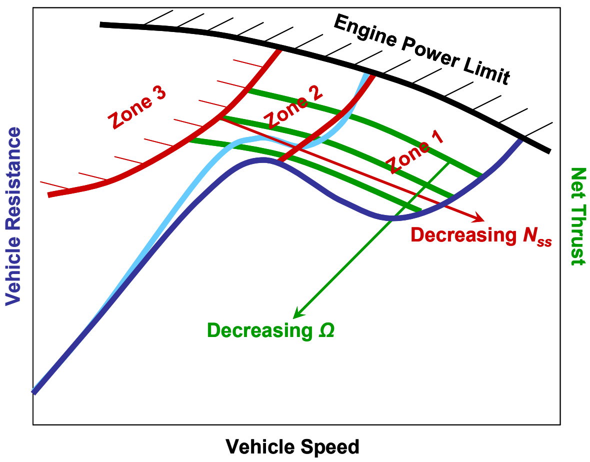

Figure B.4 Generic curves of resistance, thrust, and suction specific speed for a high-speed vessel powered by a waterjet, showing zones of operation.

In order to improve the performance and extend the operation range of vessels with waterjet propulsion, one must understand the cavitation issues, be able to better predict the occurrence of cavitation, and then improve the de- signs. In this report, the committee will first review the existing literature and discuss the cavitation issues associated with the various components of a waterjet propulsion unit. Roy (1994) presented an excellent history of waterjet propulsion units, and Wislicenus (1973) provided the fundamental hydrodynamic theory for waterjets. For work performed prior to the early 1990's, Allison (1993) gave an excellent summary of the status of waterjet propulsion. However, in recent years, commercial waterjet manufacturers have been quite secretive about their design, analysis, and testing methods and results—especially with regard to cavitation performance. Nonetheless, this literature review is still fairly extensive and representative of the technology; but it is by no means exhaustive. Finally, the committee will examine the three types of tests recommended by Hoyt et al. (1999) and the Specialist Committee on Waterjets for the 22nd ITTC, and the committee will point out where one could apply cavitation testing procedures. In addition, the committee will

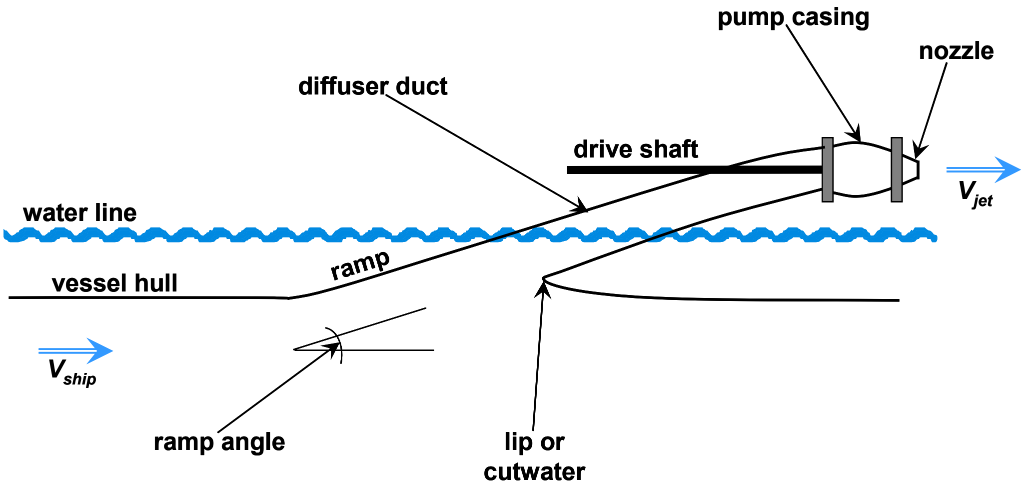

Figure B.5 Generic waterjet with a flush inlet.

recommend how some of the prediction methods discussed previously in this report can be applied to waterjets.

B.2 Waterjet Inlets

While waterjets do allow a surface vessel to operate over a large speed range, the waterjet inlet or intake must be designed to guide the flow properly through the inlet duct and into the pump, in order to achieve this range. Most waterjets today have flush inlets, as illustratein Figure B.5, while some waterjets have pod inlets, as illustrated in Figure B.6. These forward-facing pod inlets are called ram inlets, since (efficiently) bringing the water to rest downstream of the inlet would increase the static pressure to the value of the dynamic pressure. Alternately, one could compromise between a flush inlet and a pod inlet and employ a scoop, giving a partial ram inlet

Designers try to minimize the losses within an inlet to improve the overall propulsive efficiency. To minimize losses, one should also avoid flow separation under all operational conditions. Minimizing flow separation will also help avoid cavitation on the inlet surfaces. As the flow within the hull boundary layer is ingested through the inlet's "S" ducting and over the shaft, a circumferentially-non-uniform—or secondary—flow can enter the pump and degrade pump performance with regard to efficiency, cavitation, vibration, and noise. Therefore, the designer wants to minimize these flow distortions if possible. In addition, most waterjets diffuse the flow through the inlet ducting in order to increase the static pressure at the pump entrance plane and improve pump cavitation performance. However, the amount of diffusion is a trade-off between improved cavitation performance and increased losses. Finally, the inlet ducting in a vessel—and, thus, the volume of water entrained in the ducting constitutes—lost buoyancy for the vessel, so designers seek to keep the ducting as short as possible.

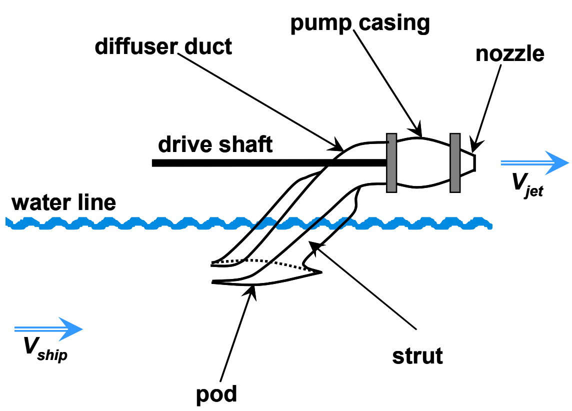

Figure B.6 Generic waterjet with a pod inlet.

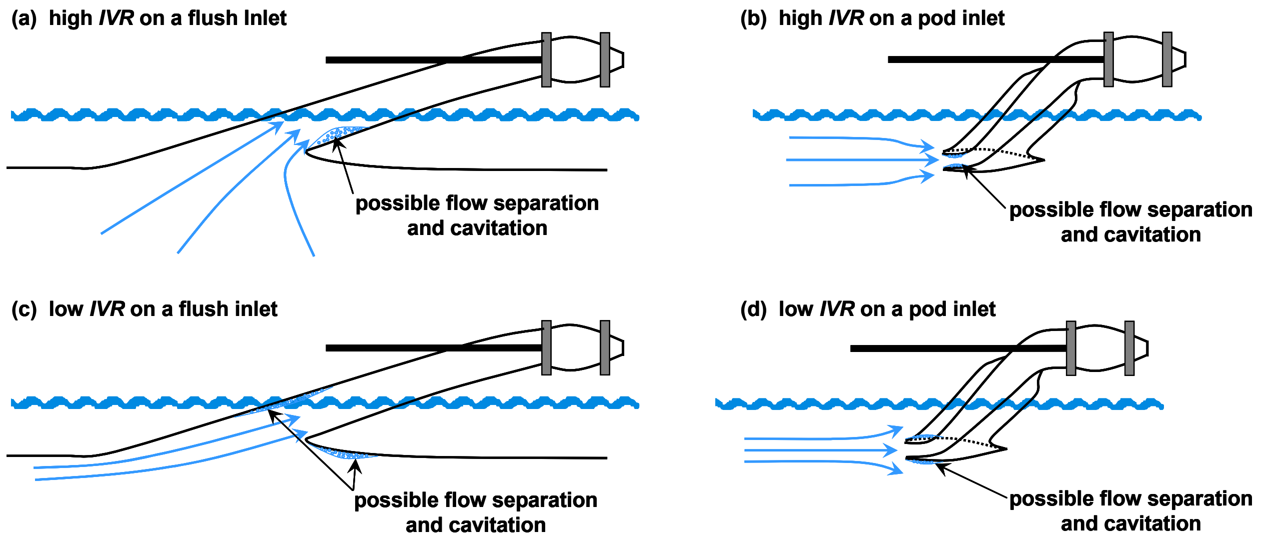

Figure B.7 Inlet flow phenomena for (a) a high *IVR* on a flush inlet, (b) a high *IVR* on a pod inlet, (c) a low *IVR* on a flush inlet, and (d) a low *IVR* on a pod inlet.

Waterjet inlets can be characterized by the inlet velocity ratio,

$$IVR = \frac{V_{pump}}{V_{\infty}}, \tag{B.1}$$

where V_{∞} is the ship speed, and V_{pump} is the average axial velocity just upstream of the pump—or the volume flow rate divided by the cross sectional area at this location. At a occur just inside of the inlet lip, as illustrated in Figure B.7(b).

At a high ship speed, or a low value of *IVR*, the flow decelerates in the inlet, relative to the flow at the design *IVR*. The resulting incidence angle for a flush inlet can lead to flow separation and cavitation on the underside of the lip or cutwater. In addition, this deceleration within the inlet can result in a significant adverse pressure gradient along the roof of the inlet, leading to possible flow separation and cavitation in this region as well. Figure B.7(c) illustrates these flow regions. Finally, Figure B.7(d) shows that—for a pod inlet—the resulting incidence angle at a low value of *IVR* can lead to flow separation and cavitation just outside of the inlet lip.

In addition to directly affecting the inlet cavitation, changes in the *IVR* will also affect the inlet losses—which affects the available

low ship speed, or a high value of *IVR*, the flow accelerates into the inlet, relative to the flow at the design *IVR*. For a flush inlet, the resulting incidence angle can lead to flow separation and cavitation on the upperside of the lip or cutwater, as depicted in Figure B.7(a). For a pod inlet, flow separation and cavitation can

NPSH for the pump and, thus, the pump cavitation.

<u>Literature Review for Waterjet Inlets.</u> English (1994) provided some practical considerations for flush inlets on waterjets. He felt that most designers use flush inlets that ingest the hull boundary layer in order to increase the ideal jet—or Froude—efficiency, thus increasing the overall propulsion efficiency. However, he points out that as this boundary-layer fluid flows through the inlet's "S" bend, it will generate a secondary flow which will be stronger for short inlet ducts with high ramp angles, which is typical. The resulting flow distortion can lead to particular forms of pump cavitation that can cause excessive vibration excitation and erosion. And even with the low inlet velocity which increases the ideal jet efficiency (and, thus, the overall propulsive efficiency), English (1994) feels that the generation of these

secondary flows can increase inlet losses, which will adversely affect the overall propulsion efficiency.

In addition, while it is both convenient and typical for inlet ducting to have a rectangular cross-section, English (1994) stated that this shape may not necessarily be the most suitable from the viewpoints of efficiency, vibration excitation, and maneuvering. Also, using principals developed for auxiliary air intakes on aircraft, he suggests the use of a scoop. And while he admits that the use of a scoop on high-speed craft may result in hull cavitation near the scoop, he feels that cavitation that is controlled and does not cause erosion on surfaces—or other problems—can be tolerated. English (1994) also suggested the use of elliptically-shaped intakes with rounded edges to help improve the flow distortion ingested into the pump. Finally, he noted the close interaction between the hull and the waterjet; where the shape of the bottom of the vehicle in the region of the intake can influence the hydrodynamic performance directly and adversely.

Steen and Minsaas (1995) stated that waterjet pump suppliers traditionally played the main role in designing the entire waterjet propulsion system for each individual ship. However, they felt that model basins were becoming increasingly involved in the design and evaluation of the waterjet system, particularly for the waterjet inlets. Based on the predicted ship resistance, Steen and Minsaas (1995) would first select the type and size of the main engine. Then, they would select an available waterjet pump to fit the engine, making sure to select the optimum jet outlet area, which determines the flow rate required to obtain the necessary increase in axial momentum and, thus, the proper thrust. Clearly, the impeller characteristics, the inlet losses, and the expected operating profile of the craft also play important roles in this design optimization process.

Next, Steen and Minsaas (1995) would design the waterjet inlet to fit the bottom of the hull, as well as considering other constraints. The cross-sectional area of the inlet mouth is of primary importance, especially when choosing the design value of *IVR* and evaluating possible regions of cavitation for off-design values of *IVR*. They developed a computer program to generate the geometry for both flush and ram inlets, using super-elliptic cross-sections and splines. The code automatically generates a mesh for a boundary-element method that allows them to evaluate the pressure and velocity distributions, as well as the risk of flow separation and cavitation. Later, they use a RANS solver to further study vortex generation and flow separation. They concluded that the inlet suction area was far from rectangular.

Steen and Minsaas (1995) also strongly advocated testing in both a towing tank and a cavitation tunnel to help design waterjet inlets without cavitation and with an optimum efficiency. For self-propulsion tests within a towing tank, they studied the waterjet/hull interaction and air ventilation into the waterjet. Even for calm water, they needed to avoid waterjet inlets with sharp corners, which lead to vortices which can draw air into the inlet. To obtain good performance for high-speed craft, it is essential to test in a seaway to design craft with as little speed loss and air ventilation as possible at higher sea states. For waterjet system tests in a cavitation tunnel, they measured the flow rate, inlet losses, and flow distortion into the pump. They also performed surface flow visualization to detect possible flow separation, and they observed cavitation on the inlet and on the impeller. They stressed the importance of observing the inlet cavitation at various values of *IVR*, as this cavitation will increase the resistance of the ship.

Seil et al. (1997) reported on the optimization of waterjet inlets using CFD. Because of the waterjet/hull interaction, they stated that the ideal optimization would include a determination of the hull form and the inlet geometry together. However, they avoided this complex hydrodynamic design problem and simply optimized the inlet geometry with an upstream turbulent, flat-plate boundary layer. They developed their own single-block, body-fitted-coordinate, structured computational grid—which they used with a commercial CFD code to solve the steady, incompressible RANS equations, with a two-equation renormalization group (RNG) k-ε turbulence model.

First, Seil et al. (1997) developed a parametric definition of the geometry for the waterjet inlet. Then, they developed a cost function based on four hydrodynamic performance parameters—the distortion of the total-pressure distribution at the exit of the inlet duct, the total-pressure loss coefficient, the volume of water entrained in the inlet duct, and the cavitation number—with coefficients and exponents to provide weighting factors for the relative importance of the four performance parameters. They used a formal optimization methodology to minimize the resulting cost function. For a given *IVR*, they ran several cases (cases with circular cross-sectional ducts), and they always found that cavitation would occur on the underside of the inlet lip. They felt that they would need to increase the radius of the inlet lip or increase the ramp angle in order to reduce the cavitation number. However, they pointed out that an *infinite* number of possible designs exist, so they could not draw many conclusions from their limited study.

Hu and Zangeneh (1999) also reported on the optimization of waterjet inlets using CFD. They also used a commercial code (with a standard k-ε turbulence model) and a body-fitted structured grid; however, they felt that they could use two-dimensional RANS solutions along the center plane for the design optimization, before checking the results with a three-dimensional RANS simulation. They performed the optimization by adjusting several B-spline control points and minimizing an cost function representing the total-pressure loss. Based on some initial geometry, they reduced the inlet total-pressure loss by 20% at the design point, with even more reduction at some off-design points. They also obtained a slightly more uniform flow at the exit of the waterjet inlet and suppressed the flow separation near the lip. However, the initial lip geometry looked very sharp, and the optimization based on two-dimensional RANS solutions provided a more rectangular cross section for the inlet duct, which may shed more vortical structures.

Bulten and Verbeek (2003) used a commercial CFD code with an in-house three-dimensional grid generator to optimize the inlet geometry of a fast ferry, a patrol boat, and a high-speed motor yacht. Their design criteria, in a priority listing, were (1) avoid flow separation under all circumstances, (2) avoid cavitation on the upper part of the cutwater at high *IVR* and on the roof at high *IVR*, (3) avoid cavitation on the underside of the cutwater at low *IVR*, and (4) minimize the volume entrained by the water within the inlet.

Brandner and Walker (2007) conducted an extensive experimental investigation of the performance of flush waterjet inlets. Within their cavitation tunnel, they fitted the inlet model to the ceiling of the test section, with an instrumented pipe length fitted downstream of the inlet to investigate flow properties at a notional pump face. Upstream of this flush inlet—which they consider typical of a conventional waterjet design—they could thicken the incoming boundary layer using a *saw-toothed fence*. They measured the static-pressure distribution along the centerline of the ramp—or roof of the inlet—and the boundary-layer profile on this surface, just upstream of the dummy, non-rotating pump rotor shaft. They also measured the static pressures on the lip to help determine the incidence angle, and they used a three-hole pressure probe to measure the flow at the exit plane of the inlet. Finally, they made observations of cavitation inception and occurrence.

As one would expect, Brandner and Walker (2007) found that the flow field within the waterjet inlet changed significantly with *IVR*. For decreasing values of *IVR*, the static-pressure gradient along the ramp became more adverse and the flow eventually separated. Secondary flow from the incoming boundary-layer fluid turning through the "S" bend dominated the flow features at the exit of the inlet, although they also saw evidence of the shaft wake and streamwise vortices shed from the square corners of the ducting. The flow became more distorted at this plane for decreasing values of *IVR*. Also, for lower values of *IVR*, the stagnation point on the lip of the inlet moved inside the duct and sheet cavitation occurred below the lip, as shown in Figure B.8. These trends in the flow field went in the other direction when increasing the values of *IVR*. At some values of *IVR*, Bandner and Walker (2007) also observed cavitation at the bottom of the duct, just upstream of the exit plane. This cavitation appeared as transient, partially-isolated, thin bubbles along the wall of the duct, with regions of coalescence.

Finally, Brandner and Walker (2007) showed inlet performance to be generally improved with the ingestion of a thicker boundary layer. The thicker boundary layer reduced the flow separation along the ramp and reduced the degree of flow distortion at the exit plane, before flow would enter the pump. However, the range of incidence angles on the lip was greater for the thicker boundary layer, increasing the likelihood of flow separation and cavitation in the vicinity of the lip.

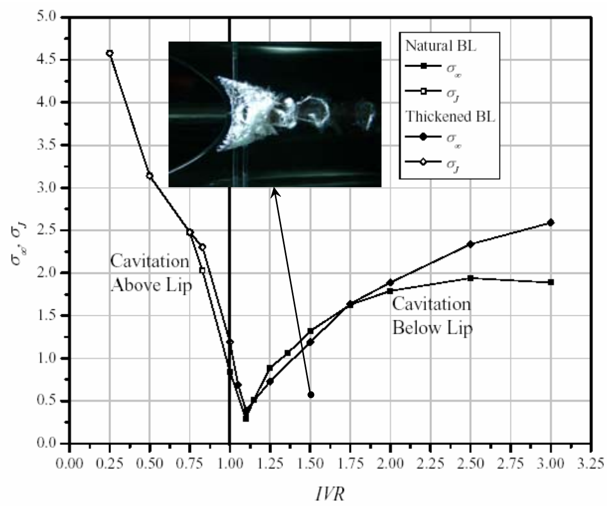

Figure B.8 Lip cavitation inception with the waterjet inlet ingesting a natural and thicknened boundary layer, as measured by Brandner and Walker (2007).

B.3 Waterjet Pumps

Historically, Allison (1993) reported that waterjet propulsion units have included pumps that range from axial-flow units, through mixed-flow units, to radial-flow (or centrifugal) units—as well as reciprocating pumps used in early waterjet propulsors. Based on similitude, one can define the specific speed, N_S , to characterize the pump type,

$$N_S = \frac{\Omega Q^{1/2}}{\left(gH^{3/4}\right)}, \tag{B.2}$$

where Ω is the rotational speed of the rotor blades, Q is the volumetric flow rate through the pump, and H is the net total head through the pump. This dimensionless parameter is independent of the size of the pump and the type of fluid. The specific speed normally defines the best hydraulic efficiency point of the pump. The approximate range of specific speeds for axial-flow pumps is 3.0-6.5, for mixed-flow pumps is 1.5-3.0, and for radial-flow (or centrifugal) pumps is 0.2-1.5. Reciprocating pumps have even smaller values of specific speed than radial-flow pumps, while propellers have even larger values of specific speed than axial-flow pumps. Propulsion systems work more efficiently with a larger flow rate and a lower total-head rise, or a higher specific speed—as indicated by Wislicenus (1973), for example—so most current waterjet propulsors incorporate either axial-flow or mixed-flow pumps.

A waterjet pump requires a minimum absolute pressure at its entrance to avoid cavitation. If the pressure at the pump face falls below this value of pressure, vapor bubbles will form, and their subsequent collapse can lead to vibration, noise, erosion, and a reduction in the waterjet thrust. This required pressure depends on the design of the inlet and the pump. Downstream of the inlet ducting, at the entrance to the pump, Wislicenus (1986) defined the total head available to the blade rows as

$$H_{sv} = \left(h_s + \frac{V_s^2}{2g} \pm \Delta z \right) - \frac{p_v}{g\rho}, \tag{B.3}$$

where h_s is the static head equal to the static pressure divided by the weight per unit volume of the fluid ($g\rho$), V_s is the fluid velocity at the place where h_s is measured, and Δz is the difference in elevation between the point where h_s is measured and the point of cavitation. This total suction head above the vapor pressure is also referred to as the net positive suction head, $NPSH$.

In his review of waterjet propulsion, Allison (1993) stated that the waterjet inlet must be capable of supplying the $NPSH$ demanded by the pump to avoid cavitation. Usually, this is no problem at the design point; but at low ship speeds, it is generally necessary to reduce power (or pump speed) to match the pump-required $NPSH_R$ to the total head available from the inlet for the existing ship speed. The available $NPSH_A$ will depend on the efficiency of the inlet.

Rather than use the cavitation number, σ, to characterize cavitation, the pump industry has used other dimensionless parameters to characterize cavitation. One of the earliest parameters is Thoma's cavitation factor (or the Thoma parameter), σ_{Th}, which can be defined simply as

$$\sigma_{Th} = \frac{H_{sv}}{H} = \frac{H_{sv}}{NPSH}. \tag{B.4}$$

Alternatively, in a manner similar to defining the specific speed, one could use similitude to define the suction specific speed as

$$N_{SS} = \frac{\Omega Q^{1/2}}{\left(gH_{sv}^{3/4} \right)} = \frac{\Omega Q^{1/2}}{\left(g \cdot NPSH^{3/4} \right)}. \tag{B.5}$$

Figure B.9 presents a generic schematic illustrating the cavitation performance of a pump, for a given flow rate. The shape and magnitude of these cavitation characteristic curves depends on the pump type (or specific speed), the details of the pump design, and the flow conditions. Various investigators characterize the degree of cavitation using σ, σ_{Th}, or $NPSH$—as shown increasing to the right on the bottom abscissa of Figure B.9—or using N_{SS}—as shown increasing to the left on the top abscissa. Figure B.9 shows three critical cavitation numbers which limit pump performance: a limit for cavitation inception, a limit for cavitation erosion, and a limit for cavitation breakdown. Note that these three critical cavitation numbers, which are usually determined experimentally, are essentially independent of one another. For instance, inception may result from cavitation in the gap between the rotor-blade tips and the casing or in the core of the resulting tip-leakage vortex—and, yet, neither of these forms of cavitation lead to erosion or breakdown on the rotor blades.

Referring to Figure B.9, if one reduces the static pressure (or the cavitation number) from a noncavitating condition, cavitation first appears at inception—typically as a crackling sound. Further reduction in static pressure leads to increases in vibration and noise. Reducing the static pressure even further results in the onset of cavitation erosion, which is caused by the implosion of vapor bubbles on the surface of the blades. This erosion rate also depends on the material of the blade.

Finally, further reductions in static pressure will lead to a major deterioration in the powering performance of the pump. The critical cavitation number for this breakdown in performance is typically defined as a 3% loss in thrust, torque, or total-head rise across the pump (although values of 2% and 5% have also been used). For axial-flow pumps, a cavity will form on the suction surface of the rotor blades, which can initially increase the blade camber—and, thus, the flow turning and blade lift—and cause a small increase in the powering parameters, as illustrated in Figure B.9. However, as the static pressure decreases towards the breakdown cavitation number, the cavity will enlarge and decrease the flow turning, causing a significant reduction in the powering parameters. For radial-flow (or centrifugal) pumps, the cavity may need to grow to the point where it *blocks* a significant portion of the impeller channel before finally resulting in performance breakdown.

Axial-flow pumps offer some key advantages within a waterjet propulsor. With a high specific speed, they provide improved efficiency. Also, their small casing diameter allows for easier installation into many existing hulls or less volume restrictions when designing a new hull. However, axial-flow pumps can have difficulty developing enough head without detrimental effects from cavitation. The three limiting cavitation numbers in Figure B.9 can be larger—or the limiting suction specific speeds can be smaller—for axial-flow pumps, although the details of the pump design and the flow condition can alter these limits. For instance, designers may increase the blade area of their axial-flow rotor blades to decrease the maximum loading or lift and improve cavitation performance, at the risk of increasing friction losses.

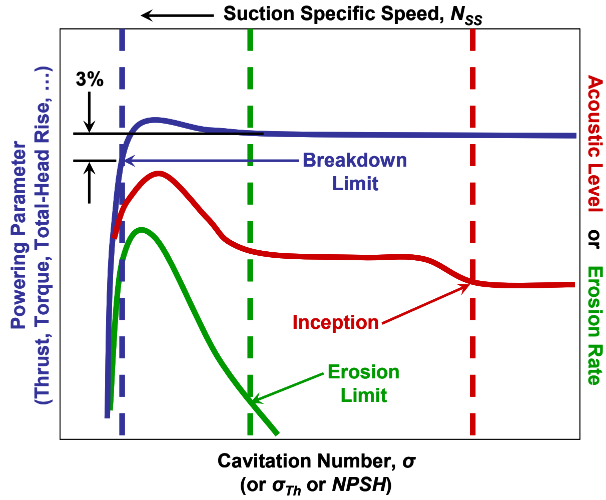

Figure B.9 Generic schematic of pump cavitation performance (for a given flow rate).

In general, pump designs with lower specific speeds will have improved cavitation performance. One possible pump type with a lower specific speed is a multistage axial-flow pump. Similar to configurations used for rocket fuel pumps, one can design an axial-flow inducer just upstream of the main impeller. This blade row will increase the static pressure to supply the $NPSH_R$ required by the impeller, without excessive loss of performance due to cavitation. Inducer blades themselves will not experience cavitation breakdown until the cavitation number becomes very small, or the suction specific speed becomes very large. Well-designed inducers will raise the static pressure gradually, without doing much work to increase the total pressure (or total head). The main impeller will perform the bulk of the work. However, the inducer—with a large blade area—will still have total-pressure losses and will lengthen the overall unit.

Another possible pump type with a specific speed lower than an axial-flow pump is a mixed-flow pump. These blade rows will provide some increase in total head through centrifugal action (an increase in radius), so the blade loading will be reduced relative to an axial-flow pump—and cavitation should be less of a problem. These pumps can still have a fairly high specific speed, but their diameter and weight will certainly be larger than those values for an axial-flow pump, providing more difficult installation issues.

Literature Review for Waterjet Pumps. Wislicenus (1973) concluded that truly cavitation-free operation within a waterjet pump requires very conservative suction specific speeds—lower than say 2.5. However, he also stated that cavitation-free operation is not always required. At increasing flow velocities within the pump, cavitation damage can increase rapidly, with damage increasing by at least the sixth power of the flow velocity, as estimated by Wislicenus (1973). Thus, an increase in flow velocity by a factor of only 1.5 will increase the rate of cavitation damage by a factor of more than ten—so even small increases in flow velocity may lead to intolerable cavitation damage.

In addition, Wislicenus (1973) discussed the cavitation issues associated with designing a waterjet to adequately traverse the "hump" speed and reach the desired cruise speed. He pointed out that one may have to design the inlet and pump for a high suction specific speed, N_{SS}, in order to get over the "hump." However, at cruise speed, this waterjet may operate at a much lower N_{SS}, and the pump may not operate completely free of cavitation, whereas a good pump designed particularly for that lower value of N_{SS} would have better cavitation performance—and probably a better efficiency as well. Given values of Q, H, and H_{sv}, the designer must then choose the value of N_{SS} to which to design his pump. Next, he can determine the shaft speed, Ω, from N_{SS}—which then determines the specific speed, N_S, and a pump type. If the designer is given a value for Ω, then he must use this value to determine both N_{SS} and N_S, and he must determine if the cavitation performance and pump type can provide an adequate design.

To achieve good cavitation performance—by choosing an adequate design value for N_{SS}—the design procedure described by Wislicenus (1973) will often give a value of N_S that suggests the use of a mixed- or radial-flow pump impeller. As an alternative, Wislicenus (1973) suggested the choice of a multistage axial-flow pump, which offers savings for weight and diameter. He described the use of a specially-designed first-stage inducer, which does have low cavitation numbers, so cavitation will occur. However, to avoid complete cavitation breakdown when designing an inducer, Wislicenus (1973) states that it is necessary to use very thin and sharp leading edges, very slight curvature of the leading portions of the blades, and somewhat larger cross-sectional areas between blades at the inlet.

Verbeek (1992) presented some basic principals for relating ship speed, pump design, and cavitation. First, he recognized that the available net positive suction head, $NPSH_A$—as determined by the waterjet installation—must exceed the net positive suction head required by the pump, $NPSH_R$. Next, following Wislicenus (1973), he showed that the suction specific speed, N_{SS}, is essentially constant for different values of specific speed, N_S, of the pump. The suction specific speed, N_{SS}, describes the flow conditions at the inlet of the pump, and Verbeek (1992) feels that commercial waterjet designs operating in a uniform flow can achieve values of 4.0 to 5.0 for N_{SS}. However, he feels that the non-uniformity of the flow at the pump inlet will lower the suction specific speed, so he used $N_{SS} = 3.5$ for his cavitation limit. Therefore, he stated that—for given loss coefficients associated with the inlet and outlet ducting—the available net positive suction head, $NPSH_R$, and the required total head, H, only depend on the inlet velocity, V_{inlet}, and the jet velocity ratio, $\mu = V_{inlet}/V_{jet}$—yielding

$$N_S \le N_{SS}\left(\frac{NPSH_A}{H}\right)^{3/4}. \tag{B.6}$$

As shown in Figure B.10, Verbeek (1992) plotted this relation to show that for a given jet velocity ratio, μ, cavitation creates an upper limit to the specific speed, N_S, of the pump as a function of ship speed. He felt that for higher ship speeds, say over 35-40 knots, the pump type should change from an axial-flow pump to a mixed-flow pump. While he does state that multistage axial-flow pumps offer an alternative to a mixed-flow pump, he stated that the trade-off gives an increased length of installation, an efficiency loss due to increased ducting, and an interaction between the stages.

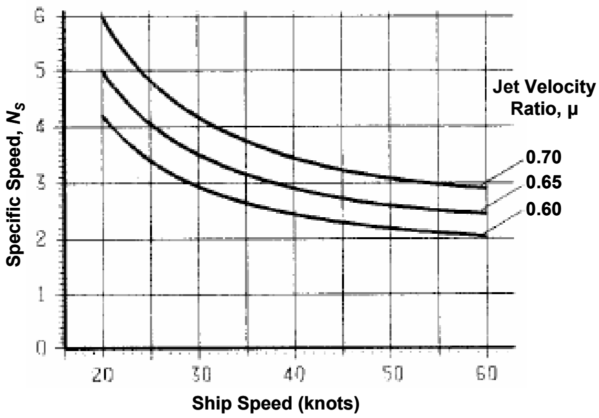

Figure B.10 Minimum required specific speed as a function of ship speed for different jet velocity ratios, as estimated by Verbeek (1992)—for a given loss coefficient of the inlet and outlet ducting.

In addition to limiting N_s and the selection of the pump type, Verbeek (1992) gave a relation showing that cavitation limits the shaft speed,

$$\Omega \le N_{SS}\left(g \cdot NPSH_A\right)^{3/4}\left[\frac{V_{inlet}(1-\mu)}{\mu \cdot T}\right]^{1/2}, \quad \text{(B.7)}$$

where T is the net thrust of the waterjet, and the velocities are integrated bulk averages. This relation shows that higher jet velocities (or lower values of μ) can allow one to increase the shaft speed while maintaining the same cavitation performance. In addition, these higher jet velocities will reduce the overall dimensions of the waterjet, with direct-drive units still a possibility. However, increasing the jet velocity too much can drastically reduce the jet efficiency—and, thus, the overall propulsive efficiency. Finally, Verbeek (1992) provides a relation to determine the specific diameter of the pump, but he cautions that experience plays a major role in determining the final dimensions.

Besides discussing the flush inlets on waterjets (as reported previously), English (1994) discussed waterjet pumps as well. He felt that the shaft speed dominates the selection of the pump type, so the choice of the main machinery—such as direct-drive diesel engines or gas turbines with gear boxes—will significantly affect both efficiency and cavitation. High shaft speeds favor smaller axial-flow pumps for improved efficiency, but making good cavitation performance more difficult to achieve.

For a propeller, the shaft inclination intensifies the flow distortion—penalizing the propulsive efficiency and causing cavitation problems such as erosion, noise, and vibration. English (1994) points out that the highly-distorted flow ingested by the highly-loaded blades within a waterjet pump creates conditions just as arduous as those of propellers, and often more so. In fact, the use of tough stainless steel for the pump parts—rotor blades (especially), stator blades, nozzle—and casing—is essential simply to survive cavitation erosion. To address this problem, he discussed attempts to improve the flow at the pump inlet plane—as discussed previously in this report—or to accept the flow distortion and improve the pump performance through design changes. For instance, he gave examples where highly-swept impeller leading edges—similar to highly-skewed propellers can attenuate vibration and noise, as well as delay cavitation erosion. For situations with very low values of *NPSH*, English (1994) gave examples of using inducers—considered to be upstream extensions to the main impeller—to create some preswirl and a small head rise. He claims that the value of

N_{SS} for cavitation breakdown can be improved by 10-20%, but he does suggest that the inducer blades should be highly swept—or highly skewed—to properly accept the distorted inflow.

Stricker, Becnel, and Purnell (1994) developed a waterjet propulsor for a vessel requiring high thrust at relatively low speeds. They included a semi-flush inlet design and a low-solidity inducer to raise the pressure to a sufficient level so that a non-cavitating *kicker* blade row can input the major part of the head rise. These two rows of axial-flow rotor blades were followed by downstream stator blades and a nozzle. Initially, they sized the waterjet using a one-dimensional optimization routine based on inducer design theory, limiting the inducer suction performance by using a flow coefficient where the *NPSH* is 20% greater than the value of *NPSH* at complete head breakdown, as determined from an experimental database. They used the mean streamline method to design the non-cavitating blade sections and used cavitating blade row theory to adjust the blade sections, choosing the incidence angles and thickness distributions to maintain their 20% margin above cavitation breakdown. Next, they used a combination of the mean streamline method and two-dimensional RANS simulations to design the *kicker* impeller blades, the stator blades, and the nozzle.

In developing an effective, compact waterjet system, Stricker, Becnel, and Purnell (1994) required an inducer flow coefficient that is typically much higher than the current practice indicated. They stated that they would further develop their optimization method to hydrodynamically integrate the inlet, jet, and hull. Finally, their development work showed them that significant waterjet performance degradation may occur due to air ingestion. For certain flush-inlet waterjet systems, they have shown that air ingestion can lead to breakdown, with very large reductions in torque and thrust.

Waterjet propulsion offers a potential advantage over conventional propellers to reduce the inboard noise of interest to passenger vessels and the underwater noise of interest to naval vessels. Aartojärvi (1995) discussed noise from waterjet propulsion—focusing on blade-frequency-related tonal noise, but also discussing jet-impingement noise and cavitation noise. As a monopole type of noise source, cavitation is an efficient noise radiator with a high-frequency noise component due to bubble collapse and lower-frequency components due to bubble oscillation, with the relative importance of these components depending on cavitation type and pressure gradients. For the non-uniform impeller inflow associated with flush inlets, Aartojärvi (1995) reported that normal conditions give rise to suction-side sheet cavitation that varies in volume depending on blade position. Under extreme conditions, suction-side bubble cavitation and pressure-side sheet cavitation may also occur. Furthermore, he reported that impeller cavitation can have a strong influence on blade-frequency noise tones due to cavitation volume pulsation. Therefore, he recommended that one designs the inlet to produce smooth circumferential wake variations and properly designs the impeller, in order to have impeller cavitation as stationary as possible. Finally, while he felt that one normally designs inlets not to have *harmful* cavitation at conditions of acceptable impeller cavitation, inlet lip cavitation may occur at off-design conditions.

In presenting a parametric method for the prediction of the powering characteristics of waterjets, van Terwisga (1997) stated that the thrust capacity of a waterjet system is governed by either the available engine power or the cavitation limits of the pump. Furthermore, he stated that the constraints limiting the impeller diameter (or waterjet size) are the available size within the afterbody of the hull and the cavitation in the pump. In developing his parametric method, he needed the resistance-speed relation for the hull form, the nozzle diameter—which is based as much on optimization of capital costs and operation costs as it is on hydrodynamics—and the specific speed of the pump—which determines the pump type, the pump efficiency, and the cavitation characteristics. Then, in developing his parametric model, van Terwisga (1997) decomposed the overall efficiency into the waterjet's freestream efficiency—which includes both an ideal efficiency and a waterjet system efficiency—and the waterjet-hull interaction efficiency. Finally, he included a parametric approach to determine the cavitation characteristics of the pump by using the suction specific speed, N_{SS}. Much of his prediction method required calibration using test data, historical empirical data, or CFD computations—especially his cavitation limitations for various values of N_{SS}.

Allison et al. (1998) gave a good summary of the tools used to design and analyze waterjet propulsors. Despite the assumptions used in one-dimensional theory, they still advocated the use of these tools for preliminary design, where they can rapidly generate performance maps based on dimensionless quantities for head, flow rate, specific speed, and cavitation number—among others. During the pump design, they advocated the use of the streamline curvature method to determine the axisymmetric flow through the waterjet. They used the mean streamline method to design the subcavitating blade sections and cavitating blade-row models to design cavitating blade sections, especially to determine the incidence angles and blade thicknesses. To account for the effect of the nonuniform inflow on cavitation performance, they stated that most designers use experience factors and developmental test data.

Allison et al. (1998) also discussed the use of lifting-surface theory to design and analyze waterjet pumps, including the coupling with a solver of the axisymmetric RANS equations. This coupling required them to extract the *effective flow field* from the RANS solution, in order to use the lifting-surface theory during the next iteration. Finally, they discussed the use of a three-dimensional RANS solver to analyze the waterjet, for both the single-phase and cavitating flow fields.

As part of the development of a commercial RANS solver, Athavale et al. (2002) developed a *full cavitation model* and applied it to three different turbomachinery applications, including a waterjet pump. This *full cavitation model* accounts for first-order effects such as phase change, bubble dynamics, turbulent pressure fluctuations, and the presence of non-condensable gasses—with several approximations required to obtain numerical results and further work required to calibrate and validate the model. One of their initial test cases involved an axial-flow pump for a waterjet, with a four-bladed inducer, followed by an eight-bladed impeller (or *kicker*), as suggested by Allison (1993). Their simulation used a 65,000-cell structured grid—with one inducer passage, two impeller passages, and three cells in the tip gaps of both blades—which is extremely coarse, especially for a viscous (turbulent) computation. However, they did show the expected increase in cavitation for a decrease in suction specific speed, N_{SS}. For the highly cavitating value of N_{SS}, they showed extreme zones of cavitation on the inducer blades, with minimal zones of cavitation on the impeller blades. Finally, they showed that the presence of non-condensable gases reduced the pump head, as well as the extent of the cavitation zone.

Carlton (2002) listed problems that he has encountered during full-scale investigations of waterjet propulsion units. His primary concerns were cavitation behavior on the pump rotor blades and cavitation erosion on the waterjet inlet lip. Cavitation on the rotor blades have led to vibration of the rotating blades and shaft, and eventually led to structural failure. He recommended designing the waterjet inlet, ducting, and pump into the hull structure in an integrated fashion.

Kooiker et al. (2003) studied the effect of *IVR* on waterjet pump performance by conducting experiments on a waterjet system mounted in a cavitation tunnel. They showed the presence of intake-pump interaction effects, which must be taken into account. The intake generates a distorted flow at the pump inlet phase and impacts pump performance. Increases in IVR—above the design value—led to increases in head coefficient and pump efficiency. Within the pump, sheet cavitation on the rotor blades was more sensitive to *IVR* than the rotor tip vortex cavitation.

In a pump test, Gowing (2005) tested a waterjet with axial-flow rotor blades followed by downstream stator blades. With a smaller diameter than a corresponding mixed-flow waterjet, this axial-flow waterjet was developed for a high-power slender-hull vessel. For three different flow rates, Gowing (2005) reduced the tunnel pressure and first observed cavitation in the rotor/duct gap and then along the leading edge of the rotor blades. He determined cavitation breakdown by measuring the total-pressure rise across the pump as he reduced the tunnel pressure. Just before the onset of cavitation breakdown, he observed a 2-3% rise in total pressure, followed by a sudden and dramatic decrease in total pressure, defining the actual onset of breakdown as the value of *NPSH* where he measured a 3% decrease in total pressure relative to the design value. Using static-pressure taps, Kiel probes, and LDV, he also acquired measurements of the flow field and compared them with CFD results.

Finally, Kerwin (2007) reviewed the waterjet design and analysis methods for inlets and, primarily, pumps. He discussed some of the methods already discussed here with a focus on RANS solvers and on a lifting-surface method coupled with an Euler/boundary-layer code, to provide a fast means of accounting for some of the viscous effects. While he did mention cavitation inception within the rotor tip-leakage vortex, he did not review cavitation modeling for either waterjet design or analysis.

B.4 Waterjet Nozzles

Cavitation within a waterjet propulsion system varies with static pressure. The low static pressure associated with waterjet inlets—which can be situated at low depths may lead to cavitation issues, especially at off-design values of *IVR*. For most waterjets, the static pressure increases as the water flows through the diffusing inlet, in an effort to improve the cavitation performance of the downstream rotor blades. The rotor blades add energy into the water and further increase the static pressure, but large local regions of strongly accelerated flow gives rise to cavitation within the rotor blades. Downstream of the rotor blades, waterjet pumps incorporate stator blades to remove the absolute swirl from the flow and raise the static pressure available to the nozzle. Well-designed blade rows will eliminate any possible hub vortex, which would certainly lead to cavitation. If a waterjet operates with no major cavitation issues on the rotor blades, the stator blades should not experience any cavitation issues—unless the rotor-blade tip-leakage vortex cavitates, and this cavitating vortex impinges on the stator blades, leading to a possible erosion issue.

Further downstream, the nozzle accelerates the flow, decreasing the static pressure to the ambient value and achieving a high jet velocity. As accelerating devices, well-designed nozzles should have small total-pressure losses. Most waterjet nozzles discharge the flow above the surface of the water—at least for higher ship speeds—although submerged, or partially-submerged, nozzles do exist. Nozzles may have a well-rounded entrance that leads to a parallel throat, such that the nozzle exit area equals the minimum jet area. However, other waterjet nozzles may simply have inner and outer peripheral walls that are straight and parallel, which leads to a *vena contracta* downstream of the nozzle exit. As pointed out by Allison (1993), it is possible for parallel-throat nozzles to experience cavitation on the nozzle walls, if they are not correctly designed.

Aartojärvi et al. (2004) showed an example of using both experiments and CFD to analyze a steering and reversing unit for a waterjet. His focus was on the static-pressure distribution, the resulting hydrodynamic forces, and estimates of fatigue life. Future analyses should address cavitation issues as well.

B.5 References

Aartojärvi, R., 1995, "Noise from Waterjet Propulsion," The 3rd International Conference on Fast Sea Transportation (FAST '05), Lübeck-Travemünde, Germany, Vol. 2, pp. 1157-1166.

Aartojärvi, R., Heder, M. Lundberg, J. and Seil, G. J., 2004, "Implementation of the Results of CFD Analysis to the Design of a New Waterjet Steering and Reversing Unit," 4th International Symposium on Waterjet Propulsion, London, Royal Institution of Naval Architects.

Allison, J. L., 1993, "Marine Waterjet Propulsion," The Society of Naval Architects and Marine Engineers (SNAME), SNAME Transactions, Vol. 101, pp. 275-335.

Allison, J. L., Jiang, C., Stricker, J. G., Athavale, M. M., Kerwin, J., and Taylor, T., 1998, "Modern Tools for Waterjet Pump Design and Recent Advances in the Field," International Symposium on Waterjet Propulsion, Latest Developments, Royal Institute of Naval Architects, Amsterdam, The Netherlands.

Athavale, M. M., Li, H. Y., Jiang, Y., and Singhal, A. K., 2002, "Application of the Full Cavitation Model to Pumps and Inducers," International Journal of Rotating Machinery, Vol. 8. No. 1, pp. 45-56.

Brandner, P. A. and Walker, G. J., 2007, "An Experimental Investigation into the Performance of a Flush Water-jet Inlet," Journal of Ship Research, The Society of Naval Architects and Marine Engineers (SNAME), Vol. 51, No. 1, pp. 1-21.

Bulten, N. W. H. and Verbeek, R., 2003, "Design of Optimal Inlet Duct Geometry Based on Vessel Operational Profile," The 7th International Conference on Fast Sea Transportation (FAST '03), Ischia, Italy, Vol. I, Session A2, pp. 35-40.

Carlton, J. S., 2002, "Waterjet Propulsion: Some Recent Full-Scale Experience," Proceedings of the 2nd Pusan National University Colloquium, Pusan, South Korea.

English, J. W., 1994, "Practical Considerations on Waterjets with Flush Intakes," International Symposium on Waterjet Propulsion, Latest Developments, Royal Institute of Naval Architects, London

Garrett, J. H., 1967, "Comparison of Three Theories of Water-Jet Propulsion," U.S. Navy Marine Engineering Laboratory, Technical Memonrandum 484/66.

Gowing, S., 2005, "CCDoTT Waterjet Pump Test in the 24" Water Tunnel," Naval Surface Warfare Center Carderock Division (NSWCCD), Hydromechanics Department, Technical Report, NSWCCD-50-TR-2005/103.

Hoyt III, J. G. (Chairman), 1999, "Report of the Specialist Committee on Waterjets," 22nd ITTC, Seoul, South Korea and Shanghai, China, pp. 587-613.

Hu, P. and Zangeneh, M., 1999, "A Method for Automatic Optimisation of the Intake Duct Geometry of Marine Water-Jets," The 5th International Conference on Fast Sea Transportation (FAST '99), Seattle, Washington, United States, pp. 843-851.

Kerwin, J. E., 2007, "Hydrodynamic Issues in Waterjet Design and Analysis," Keynote Lecture, Proceedings of the 26th Symposium on Naval Hydrodynamics, Rome, Italy.

Kooiker, K., van Terwisga, T., Verbeek, R., and van Terwisga, P., 2003, Performance and Cavitation Analysis of a Waterjet System in a Cavitation Tunnel," The 7th International Conference on Fast Sea Transportation (FAST '03), Ischia, Italy, Vol. I, Session A1, pp. 57-62.

Kruppa, C. (Chairman), 1996, "Report of the Specialist Committee on Waterjets," 21st ITTC, Trondheim and Bergen, Norway, pp. 189-209.

Roy, S. M., 1994, "The Evolution of the Modern Waterjet Marine Propulsion Unit," International Symposium on Waterjet Propulsion, Latest Developments, Royal Institute of Naval Architects, London.

Seil, G. J., Fletcher, C. A. J., and Doctors, L. J., 1997, "Optimisation of Waterjet Inlets Using Computational Fluid Dynamics," The 4th International Conference on Fast Sea Transportation (FAST '97), Sydney, Australia, Vol. 1, pp. 59-64.

Steen, S. and Minsaas, K. J., 1995, "Experiences from Design and Testing of Waterjet Inlets for High Speed Craft," The 3rd International Conference on Fast Sea Transportation (FAST '95), Lübeck-Travemünde, Germany, Vol. 2, pp. 255-1270.

Stricker, J. G, Becnel, A. J., and Purnell, J. G., 1994, "Some Important Factors in Development of Waterjet Systems," International Symposium on Waterjet Propulsion, Latest Developments, Royal Institute of Naval Architects, London, Great Britain.

van Terwisga, T. J. C., 1997, "A Parametric Propulsion Prediction Method for Waterjet Drive Craft," The 4th International Conference on Fast Sea Transportation (FAST '97), Sydney, Australia, Vol. 2, pp. 661-667.

van Terwisga, T. J. C. (Chairman), 2002, "Report of the Specialist Committee on Validation of Waterjet Test Procedures," 23rd ITTC, Venice, Italy, Vol. II, pp. 379-407.

van Terwisga, T. J. C. (Chairman), 2005, "Report of the Specialist Committee on Validation of Waterjet Test Procedures," 24th ITTC, Edinburgh, United Kingdom, Vol. II, pp. 471-508.

Verbeek, R, 1992, "Application of Waterjets in High-Speed Craft," *Hydrodynamics: Computations, Model Tests and Reality*, Proceedings of MARIN Workshops on Advanced Vessels, Station Keeping, Propulsor-Hull Interaction, and Nautical Simulators, Maritime Research Institute Netherlands (MARIN), Wageningen, The Netherlands.

Wilson, M. B., Hoyt III, J. G., Scherer, J. O., Gorski, J. J., and Becnel, A. J., 2003, "The Gulf Coast Waterjet Design and Experimental Evaluation Project for a Small Navy Ship," SNAME Propeller/Shafting 2003 Symposium, Virginia Beach, Virginia, pp. 18-1~18-19.

Wislicenus, G. F., 1973, "Hydrodynamic Design Principles of Pumps and Ducting for Waterjet Propulsion," Report 3990, Department of the Navy, Naval Ship Research and Development Center, Bethesda, Maryland.

Wislicenus, G. F., 1986, "Preliminary Design of Turbopumps and Related Machinery, NASA Reference Publication 1170, National Aeronautics and Space Administration, Scientific and Technical Information Branch.